TESTING AND SIMULATION OF THE SRF WAFER TEST CAVITY FOR THE CHARACTERIZATION OF SUPERCONDUCTORS AND HETEROSTRUCTURES

A Thesis

by

JUSTIN KYLE COMEAUX

Submitted to the Office of Graduate and Professional Studies of
Texas A&M University
in partial fulfillment of the requirements for the degree of

MASTER OF SCIENCE

Chair of Committee,	Peter McIntyre
Committee Members,	Alexey Belyanin
	Robert Nevels
Head of Department,	George Welch

August 2014

Major Subject: Physics

ABSTRACT

The wafer test cavity, designed at Texas A&M University, has been constructed and tested at Thomas Jefferson National Accelerator Facility. The mode structure, quality factor and coupling methods have been investigated. The TE_{011} mode has been located at 1.886492 GHz and the quality factor has been measured from room temperature to 2K. The measured quality factor at 2.7K is found to be 3.96×10^8. Simulations of the cavity have been performed using Comsol Multiphysics and Mathematica to demonstrate the cavities potential as a test bed for superconducting materials, such as Heterostructures. The results of the experimental measurements are incorporated into the simulations to show that a Radio Frequency magnetic field of 162 mT can be placed on a sample of superconducting material, giving 81% of the BCS critical magnetic field for niobium.

TABLE OF CONTENTS

Page

LIST OF FIGURES

Page

I. INTRODUCTION AND LITERATURE REVIEW

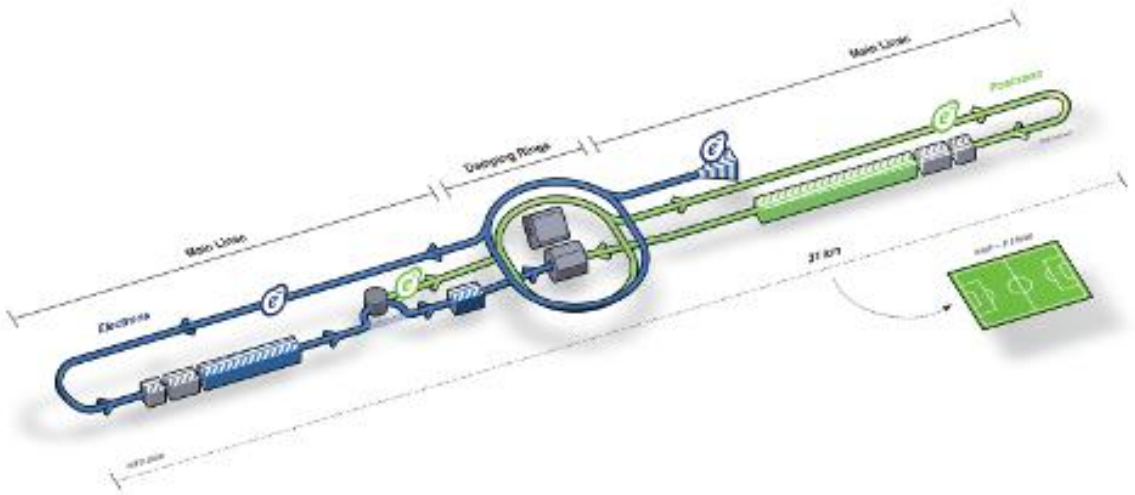

Figure 1: Layout of the International Linear Collider

Superconducting Radio-Frequency (SRF) cavities have seen considerable advancement with higher gradients and higher quality factors. The next generation particle accelerators depend on ever higher gradients and lower operating costs, as a staple of their design. For example, the International Linear Collider, pictured in Figure 1, is now designed to have an operating gradient of 31.5 Megavolts per meter, using 16,000 superconducting cavities operating at a temperature of 2K [1]. While many accelerators currently employ superconducting technology, the need for higher performance and lower costs is always present.

Some of the systems currently employing SRF technology include the Continuous Electron Beam Accelerator Facility (CEBAF) at Thomas Jefferson National Accelerator Facility [2]; the Spallation Neutron Source (SNS) at Oak Ridge National Laboratory [3]; the Large Hadron Collider (LHC) at CERN [4]; the Diamond Light

Source [5]; The Free Electron Laser User Facility (FLASH) at DESY [6]; Soreq Applied Research Accelerator Facility (SARAF) at Soreq [7] and several other facilities. The next generation of light sources also rely on SRF technology, such as the Linear Coherent Light Source II (LCLS-II) at SLAC [8] and the European X-ray Free Electron Laser (X-FEL) at DESY [9].

The above facilities almost exclusively use niobium to construct their cavities. The reason for this is that niobium has the highest elemental critical temperature and has had considerable effort put into construction techniques. This makes it difficult for new materials to gain any traction, as niobium is deeply rooted in the SRF and accelerator communities. The vast majority of effort has gone into the development of improved manufacturing and cleaning techniques, but these only offer marginal return on their investment. The SRF and accelerator community could benefit greatly from the introduction of higher performance superconductors, such as Nb_3Sn or MgB_2. The problem with these materials is that they require more preparation of the materials and different preparation techniques from niobium. The development of these conductors and techniques could be sped up drastically by having the capability to validate the materials on a smaller, more cost effective scale. Similar to the short sample tests that the superconducting magnet community employs, we have proposed and constructed an SRF cavity for just this purpose. While this is not a novel idea, I intend to prove that the wafer test cavity can perform this function more effectively than previous cavities. In collaboration with Thomas Jefferson National Accelerator Facility (TJNAF), we have constructed and performed a round of testing using niobium as a sample material.

In this thesis I will provide a background on why the wafer test cavity was designed and constructed. Followed by computer simulation, using Comsol Multiphysics and Mathematica, which will illustrate what information should be seen and what properties of the material in question can be derived. Finally I will present the testing and evaluation that took place at TJNAF and compare these results with the simulation performed.

II. DESIGN AND SIMULATION

II.I. Cavity Applications

Niobium is the material of choice for SRF accelerating cavities, which are used in the majority of particle accelerators with energies above tens of MeV. Niobium has the highest critical temperature of any elemental superconductor, simplifying manufacturing and processing compared to composite materials and alloys. This feature makes niobium cavities considerably cheaper to produce, since there is a simpler manufacturing process, as compared to Nb3Tn or MgB2. We are currently reaching the limitations of niobium as the community has pushed for higher accelerating gradients thus requiring higher surface RF magnetic fields. These designs have reached the critical field of niobium, which is 200 mT [10]. Given that a substantial amount of effort has gone into the electromagnetic design of these cavities, we must look for new materials to increase the performance of accelerating cavities, and identify the limiting criteria that can inhibit niobium's performance. This performance is necessary for the next generation of accelerators and will enable the upgrade of existing facilities.

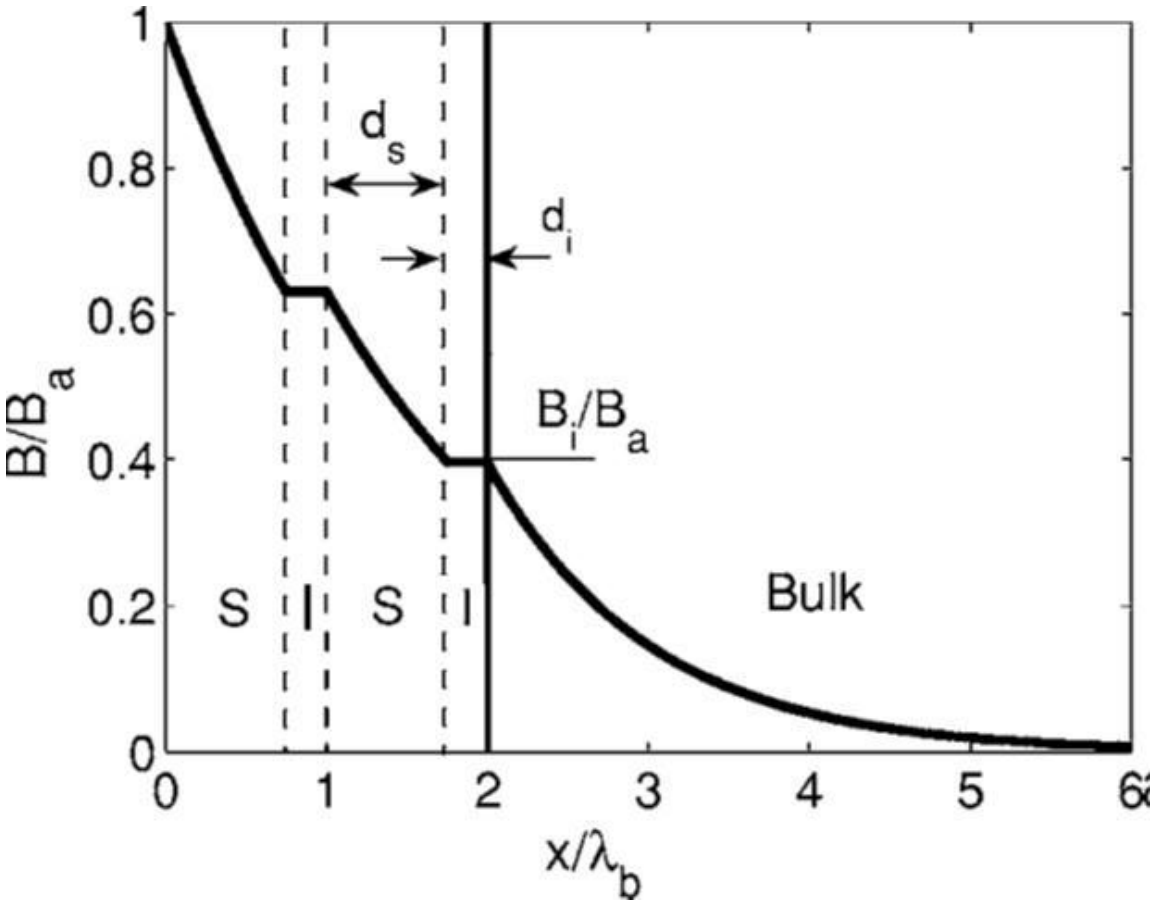

Figure 2: Magnetic Field Distribution as a Function of Depth in the Conductor

The wafer test cavity was designed and constructed to provide a systematic means to test materials with different preparations and new candidate materials to supplement or replace bulk niobium as the material of choice for SRF cavities [11, 12]. Heterostructures, theorized by Alex Gurevich, offer a solution to the issue of the critical RF magnetic field [13]. The structure consists of layered superconductor and insulator, where superconductors with higher critical field are used to "step down" the magnetic

field to a level the bulk niobium can sustain. Figure 2 shows a plot of the relative magnetic field versus the depth in the conductor. This shows how the material layers are used to reduce the field in the bulk niobium, and how they could be used as coatings on bulk niobium to create higher performance cavities. The issue with these structures is that they are complicated to manufacture and require sophisticated techniques. This is by no means a show stopper that would prevent the use of these materials, but it does present a problem in testing cavities made with these techniques. Development is also necessary for cavities coated or constructed from Nb_3Tn [14] and MgB_2 [15]. Both of these materials will be useful in the implementation of heterostructures and offer higher performance in their own rights. Though, it is expensive to construct an SRF cavity and the cost gets considerably higher when you have to build a new cavity for each step of progress in the manufacturing research. This is where the wafer test cavity becomes a necessary tool for developing new superconductors. The idea behind this cavity is to be able to perform measurements on material samples that are smaller and simpler than an entire SRF cavity. This type of tool would allow for a much more rapid development of materials and processing techniques.

II.II. Previous Cavity Designs

The concept for building a cavity to be used as a test bed for superconducting materials is not original to the wafer test cavity. Several cavities have been designed and constructed, with varying degrees of success. The previous cavities have had limitations on the size of the sample and the magnetic field strength that can be placed on the sample. These two ideas are connected in that the ideal cavity would be constructed of

niobium, as it is similar in characteristics to the materials of interest and its properties are well understood. The issue with using niobium as the material for the cavity is the obvious limitation on the magnetic field, due to niobium's critical field limit. A method has been developed to deal with this issue and it will be presented in the design section of this thesis.

Over 16 TE_{011} mode cavities have been built for the purpose of testing new materials and a list, complied by Dr. Charlie Reece, of some of these cavities and the properties of interest are presented in graphs shown by Dr. Nathaniel Pogue [11] and Dr. Binping Xiao [16] . Both present a thorough list of previous materials test cavities, so only a couple of examples will be presented here. The first cavity of interest influenced the mushroom shape of the wafer test cavity and it was utilized at SLAC. The second example is the Surface Impedance Cavity (SIC), currently in use at TJNAF.

The SLAC test bed for superconducting materials is a mushroom shaped cavity that operates in a TE_{013}-like mode that is in the X-band at 11.424 GHz [17]. This mode was selected under the premise that it doesn't have any surface electric fields, which would cause multipacting in the cavity. The profiles for the electric and magnetic fields are presented in Figure 3. The cavity is designed to have a 75% higher surface magnetic field on the bottom sample plate than on the surface walls of the cavity. The issue with higher fields is that there is a spot on the curved wall of the cavity that has field strength of ~57% of the maximum field. This cavities shape influenced the shape and design of the wafer test cavity.

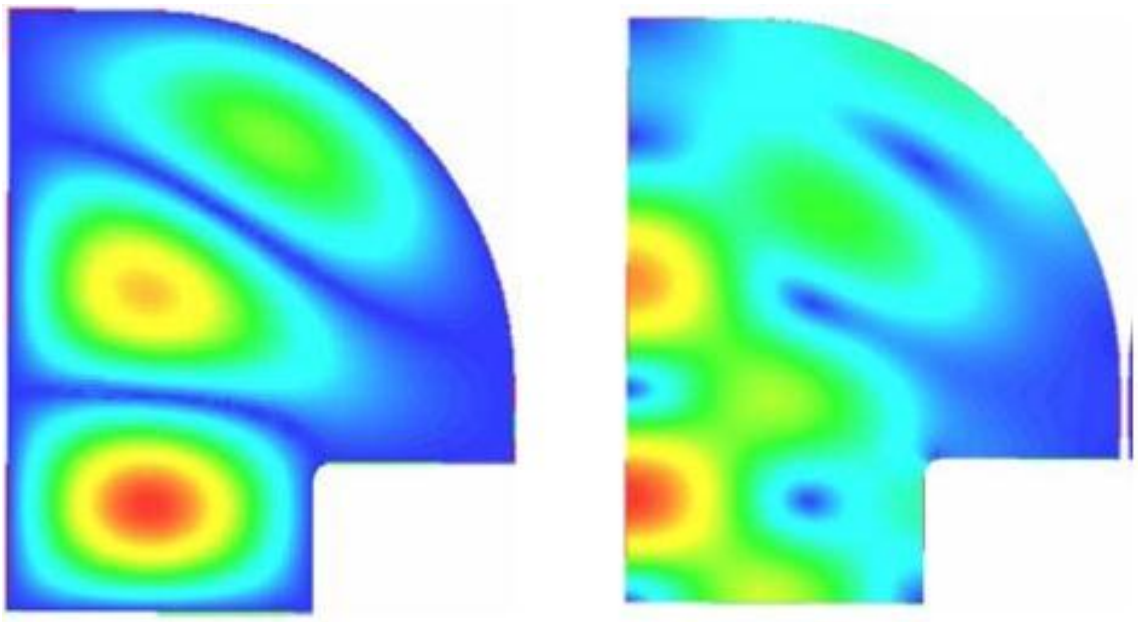

Figure 3: SLAC Mushroom Cavity Electric Field (Left) and Magnetic Field (Right) Plots

The Surface Impedance Characterization cavity (SIC) [16, 18, 19] is also of interest as it provided the predecessor to using a dielectric lens for focusing the fields onto the sample. The SIC cavity is a 7.5 GHz, sapphire loaded, TE_{011} cavity that provides a means to measure the surface impedance of a superconducting sample using calorimetric measurement techniques on the sample. A schematic view of the SIC cavity is provided in Figure 4.

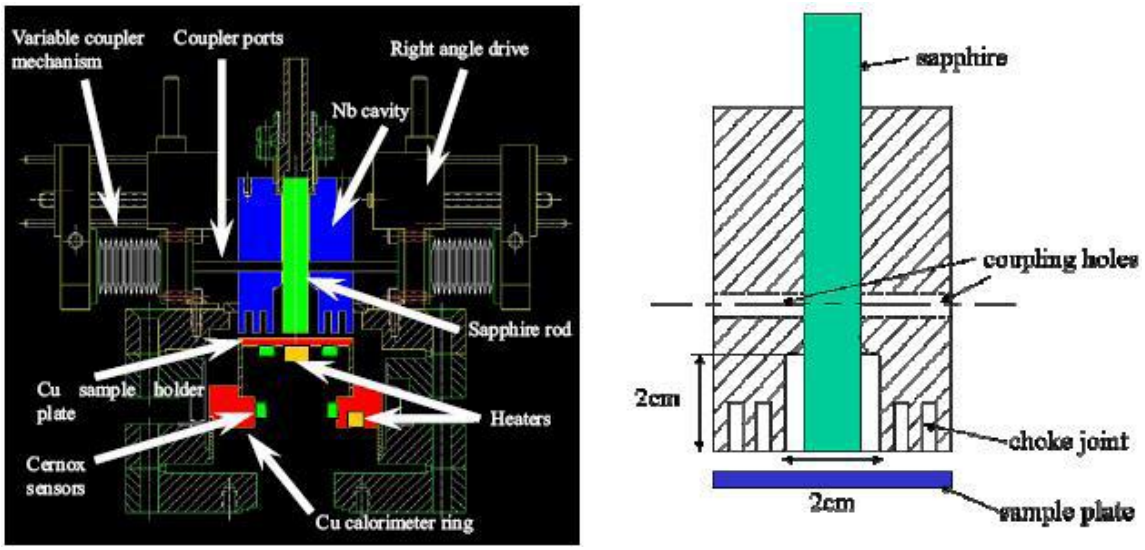

Figure 4: Surface Impedance Characterization Cavity Mechanical Layout

The cavity is designed with a sapphire concentrator onto a sample plate, which is thermally isolated from the rest of the cavity. The thermal isolation allows for the sample to be heated and have cernox resistors placed on it for measurements. Choke joints are used to contain the majority of the RF field on the sample plate. Recent results from the SIC cavity have given valuable data on many different types of samples [20], though the low magnetic field and high frequency leave room for improvement. An issue noted in [11] is that at or above 7 GHz, impurities in the sapphire give rise to paramagnetic resonances, which degrade the loss tangent of the sapphire. At lower frequencies these resonances disappear, which allows for ultimately higher fields in the cavity.

II.III. Cavity Design

The wafer test cavity was designed to be used as a test bed for novel superconducting materials. The cavity was designed by N. Pogue, P. McIntyre, and A. Sattarov from Texas A&M University and C. Reece from TJNAF [21].

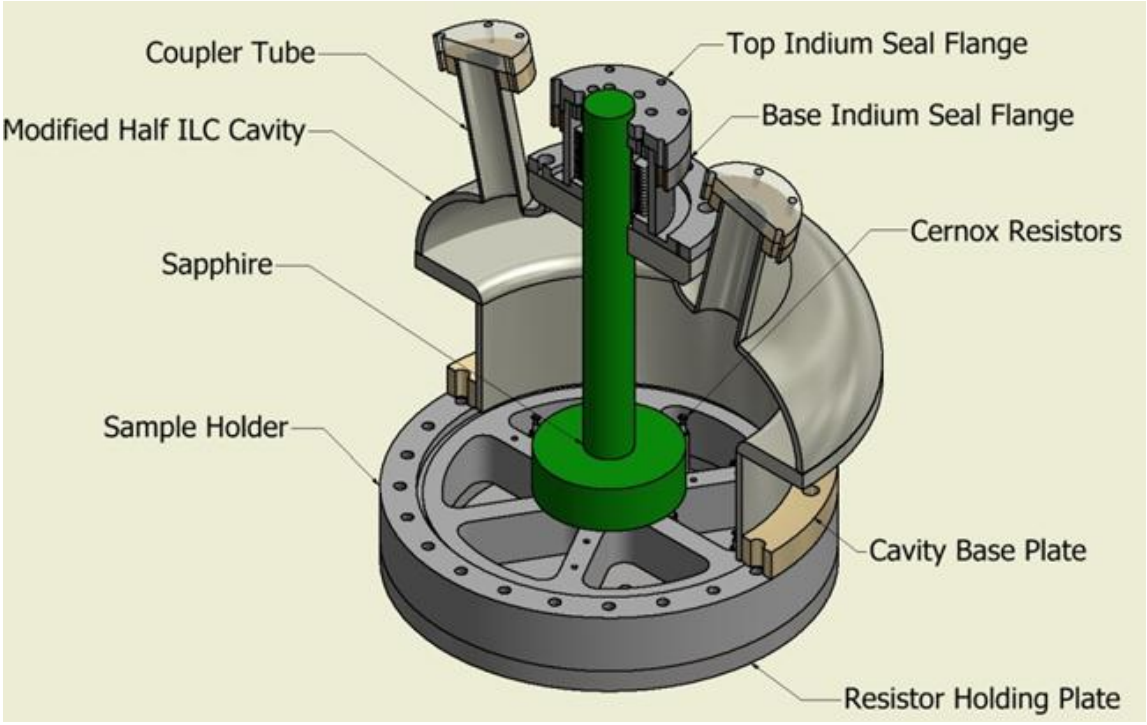

Figure 5: Wafer Test Cavity Layout

A schematic cross section of the wafer test cavity is shown in Figure 5. The sample is placed onto of the sample holder and then bolted to the cavity base plate to seal the cavity. RF power is introduced into one of the coupler tubes and a probe is placed in the other tube to measure the transmitted power. These quantities, combined

with other measurements give valuable information on the sample in the cavity, which will be described in later sections.

The cavity was designed to have an RF magnetic field on the sample surface that could be approximately 9 times the critical RF magnetic field of niobium, so that higher performing materials could be tested in the cavity. This poses a problem, as the cavity is constructed from niobium, so the field must be concentrated on the sample where it does not reach the walls of the cavity. This is achieved by using a pure single crystal Hemex sapphire by Crystal Systems as a dielectric lens, pictured in Figure 6, where the electric field in concentrated in the sapphires bottom edges. This places the highest magnetic field near the samples surface. In Figure 7, a model of the cavity is shown, with the sapphire region highlighted. Figure 8 shows the magnetic field present in the cavity, where the highest concentration is in the sapphire itself. In this model, the maximum surface magnetic field in the cavity is 9.02 times higher than the surface field anywhere else in the cavity. The magnetic field distribution is achieved by manipulating the electric field in the cavity, by placing a large portion of the sapphire in the region of interest of the cavity.

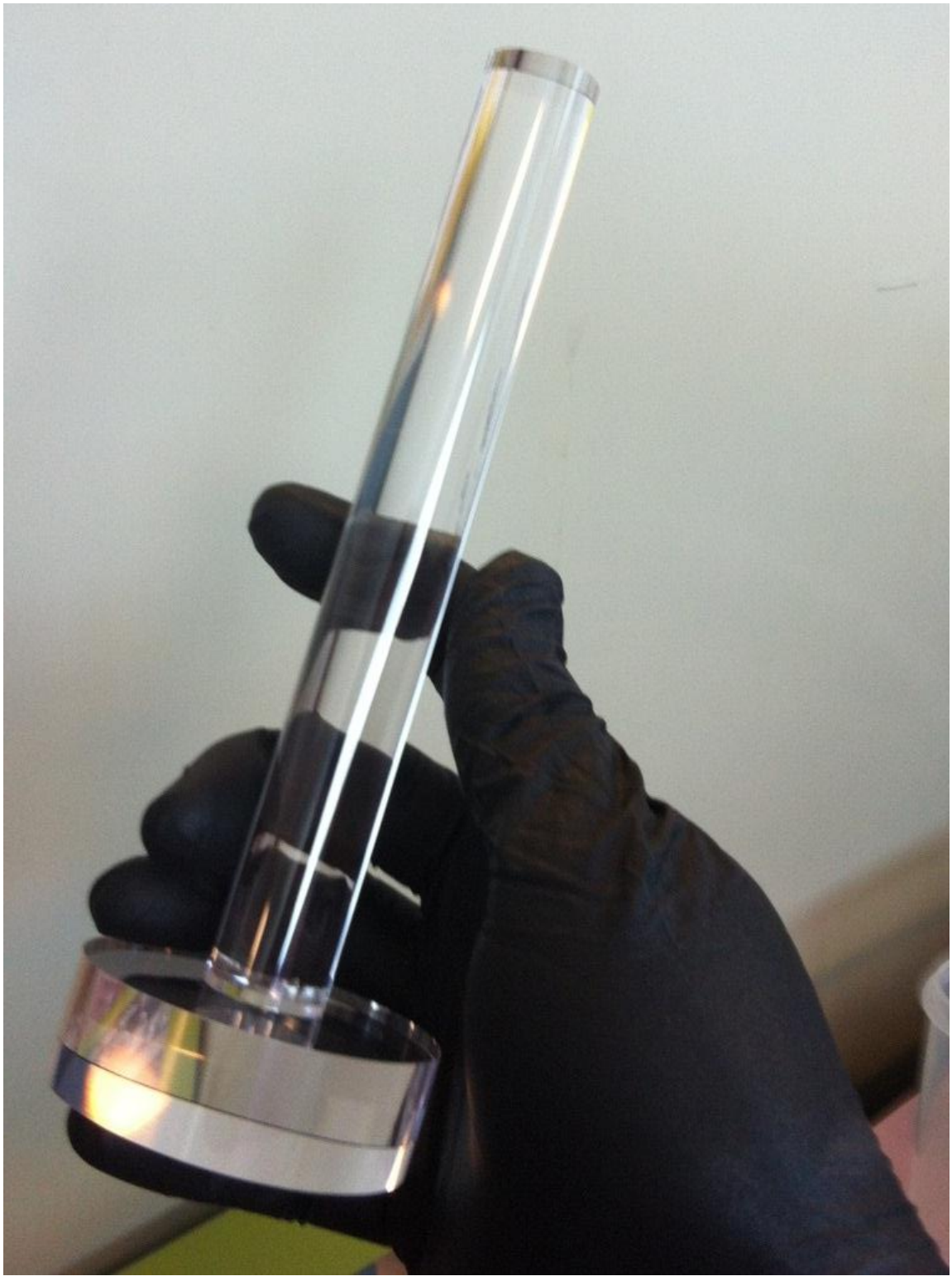

Figure 6: Single Crystal Hemex Sapphire, Sourced from Crystal Systems

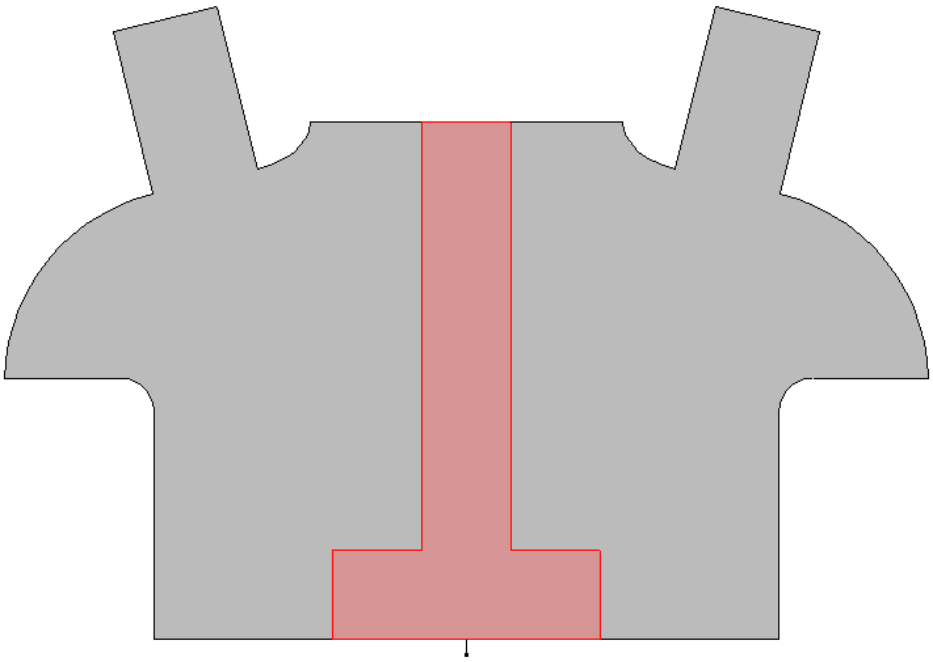

Figure 7: 3 Dimensional Comsol Model Layout, With Sapphire Crystal in Red

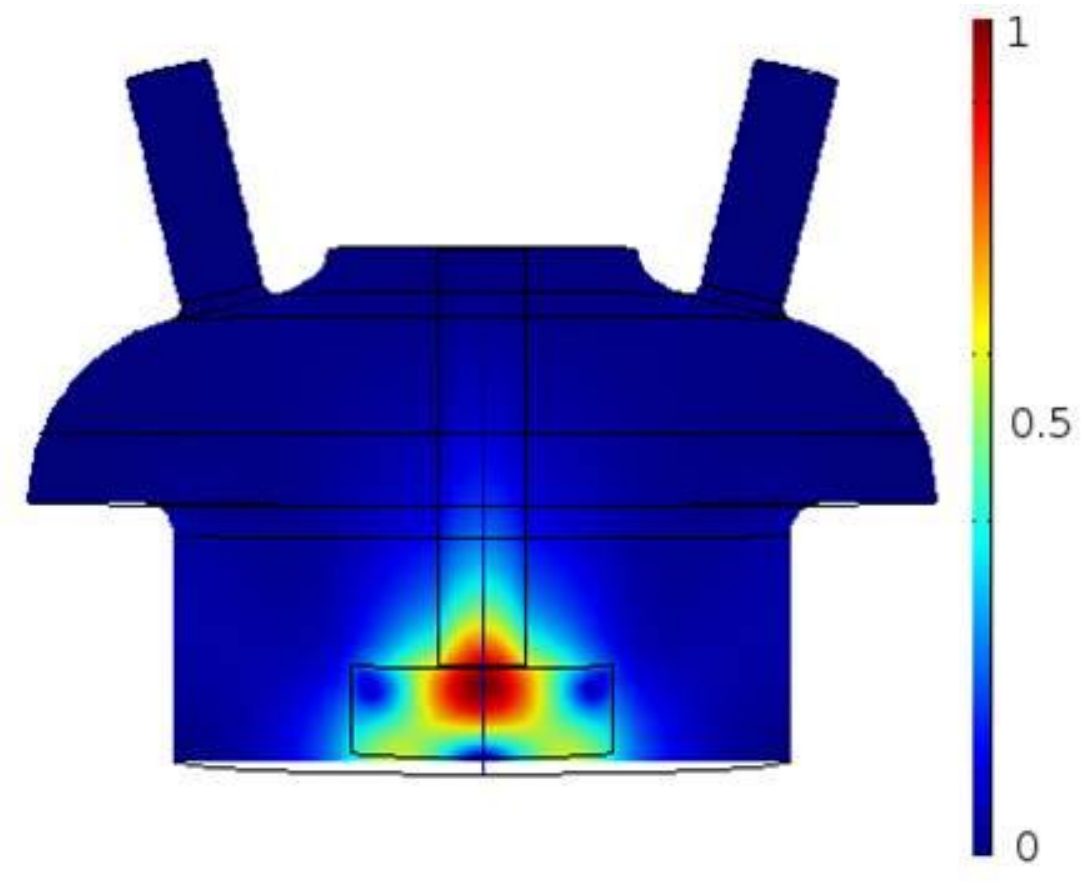

Figure 8: Comsol Magnetic Field Plot, Normalized to Peak Magnetic Field of Unity

A more detailed explanation of the modeling that was done on the wafer test cavity is presented in the following sections, but it is useful to see the field maps to follow the design process of the cavity. In the testing and modeling that were performed for this work, the sapphire was suspended 0.5 inches above the sample niobium plate in the cavity, which gives a 5 to 1 ratio of sample to wall magnetic field. This was done in order to locate the mode of interest with a high degree of certainty and maintain that

mode to allow results from multiple tests to be compared to one another. Normally there are methods of perturbing a field, by changing the couplers for instance, that would allow one to find the mode of interests easily and with certainty. An issue that was encountered in the wafer test cavity is that the couplers are recessed into tubes to prevent them from perturbing the field within the cavity, which makes it difficult to accurately identify the TE and TM modes. The coupler section of the testing chapter will show how we addressed with issue and how it led to the setup that was used for the testing of the cavity.

II.IV. Comsol Modeling

Initial modeling for the cavity was performed using Comsol Multiphysics. The mode structure and fields was investigated using an eigenmode solver within the RF package. This allowed for modeling of the magnetic field to determine the peak magnetic field relative to the fields within the rest of the cavity. Again, the cavity was designed before the start of the work being presented here, initial modeling is covered in [11]. Simulation for this work began by mapping out the mode structure, first with the crystal resting of the sample and then as a function of height over the sample. The purpose of this initial simulation was to determine how to best to experimentally confirm that we were observing the TE_{011} mode, as it is the mode of interest. In an accelerating cavity for instance, it is possible to orient a coupler to either couple to TE or TM modes, which allows relatively easy identification of modes, as the lower order modes are of most interest. The issue with the wafer test cavity was that we are interested in the fundamental TE mode, which has several TM modes below it. The couplers are recessed

into tubes, to prevent field perturbation, which makes identifying the exact mode difficult.

The number of degrees of freedom varies from simulation to simulation, but for a given model the number of degrees of freedom solved for is 290452. This is for a fully 3 dimensional model that has been imported from Autodesk Inventor using drawings originally done by Raymond Garrison and modified by Chase Collins. The average time for a solution again varies quite substantially, but the above quoted model took 43 seconds to solve, using a laptop with a Core i7 processor with 16 gb of ram.

Modeling of the cavity began with a considerably smaller 3 dimensional model acquired from previous work done from Dr. Pogue. This was done by taking the cavity geometry and assuming that it is completely symmetric and taking on a sliver of the entire cavity. This did two favorable things for modeling the cavity, first being that it made the model considerably smaller and second it allowed us to impose boundary conditions to investigate specific modes. Figure 9 shows the side and top view of the geometry used in the sliver model, where the sapphire is in red. Figure 10 and Figure 11 illustrate the electric and magnetic field distributions of the sliver model, respectively. This model gives a resonant frequency of 2.221 GHz for the TE_{011} mode, with the sapphire positions touching the bottom region. The optimum height of the crystal, above the sample, was of much discussion during the build up for the testing of the cavity, but was ultimately not necessary due to the issues involved with finding the correct mode. This modeling was still useful as a quick check for any future modeling and gave a reference which could be compared to previous work done on the design of the cavity.

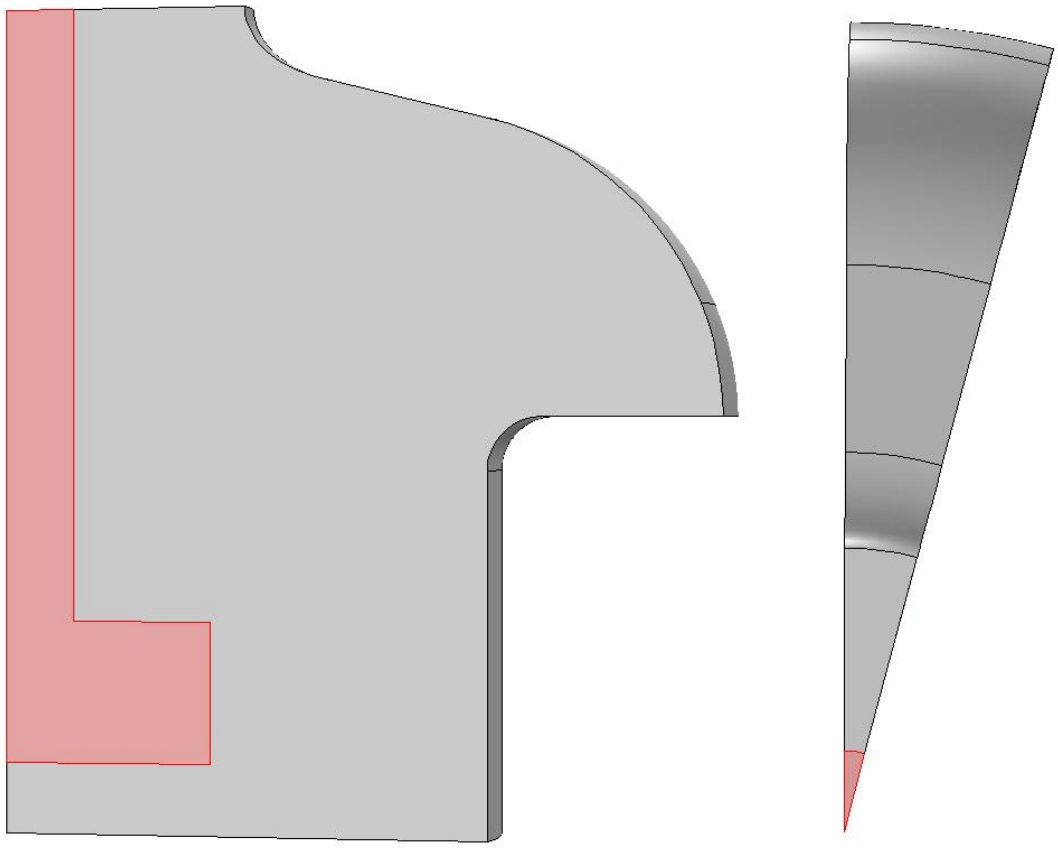

Figure 9: Comsol Sliver Model Layout, With Side (Left) and Top (Right) Views, the Sapphire Crystal is in Red

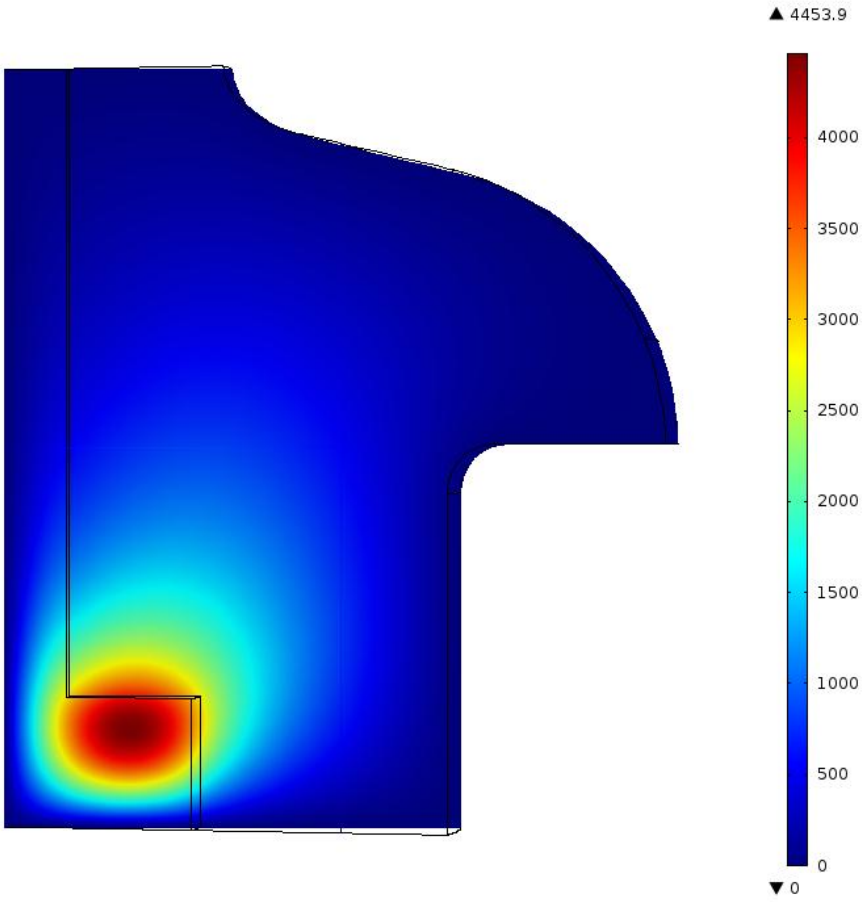

Figure 10: Comsol Sliver Model Electric Field Plot

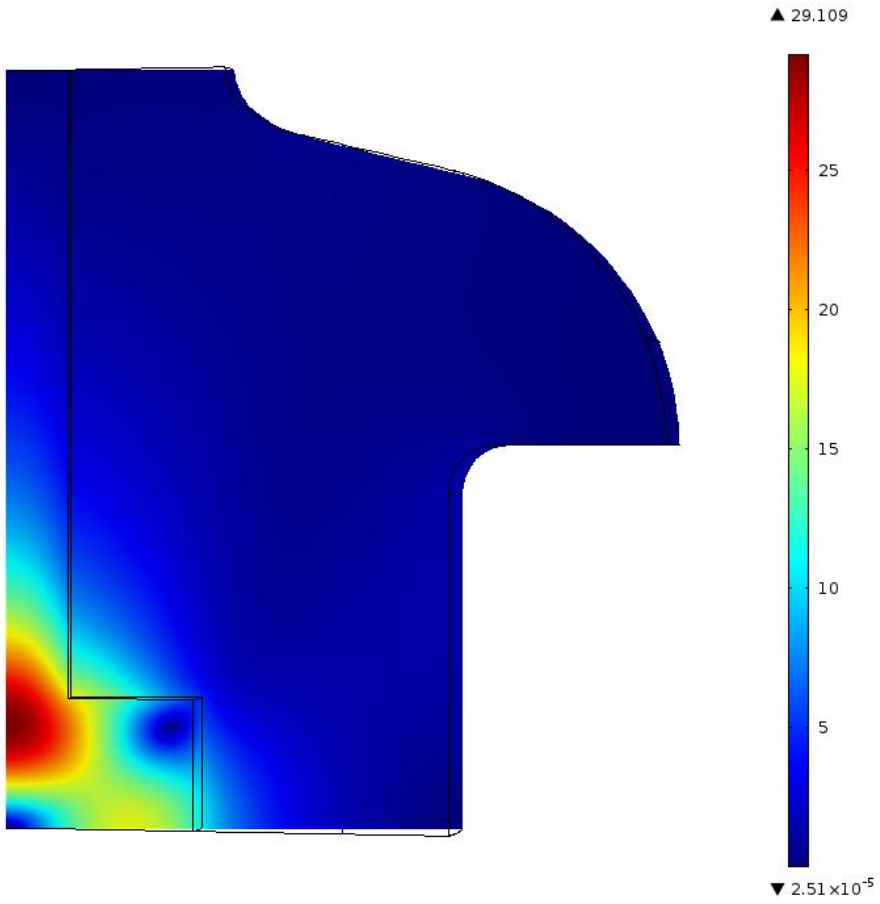

Figure 11: Comsol Sliver Model Magnetic Field Plot

The following set of simulations was performed with the intent of finding the best method for conclusively finding the mode of interest. This was done by first finding the relative quality factor of the mode of interest versus the other closely lying modes. A parametric model was constructed, where the height of the crystal above the sample was swept from 0 to several inches in height. This allowed for the comparison of frequencies versus the crystal height, a plot of which is provided in Figure 12. This information was

useful experimentally for two reasons. First it can be seen that the TE_{011} mode is the only mode to shift past other modes. The second reason is that it allowed us to pick a crystal height which maximized the distance, in frequency, between other modes to ensure the correct mode was observed. A representative set of pictures is presented in the previous section, which shows the model layout, electric and magnetic field distributions.

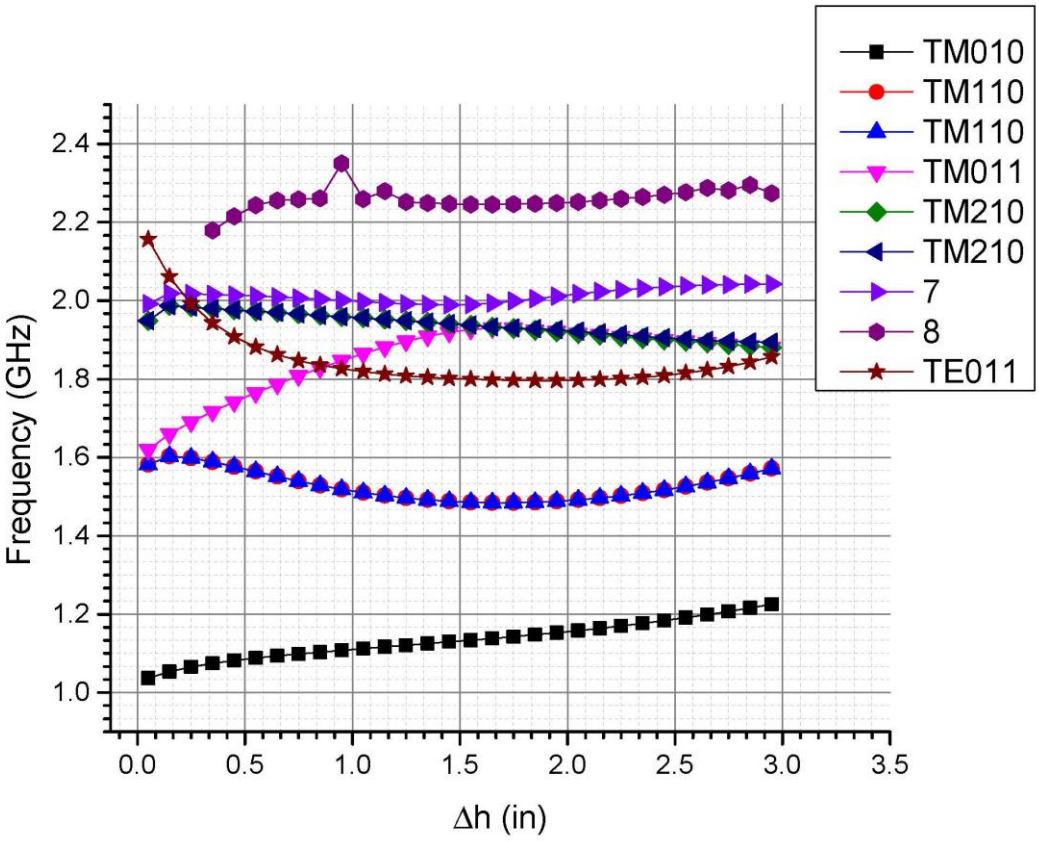

Figure 12: Frequency versus Crystal Height for the First 8 Modes, TE_{011} Mode is Shown in Red with Star Markers

This same parametric model was also used to predict the quality factor of the modes modeled, while the cavity was at cryogenic temperatures. This information was

also used to ensure the correct mode. A graph of the quality factor of the modes versus the height of the crystal is presented in Figure 13.

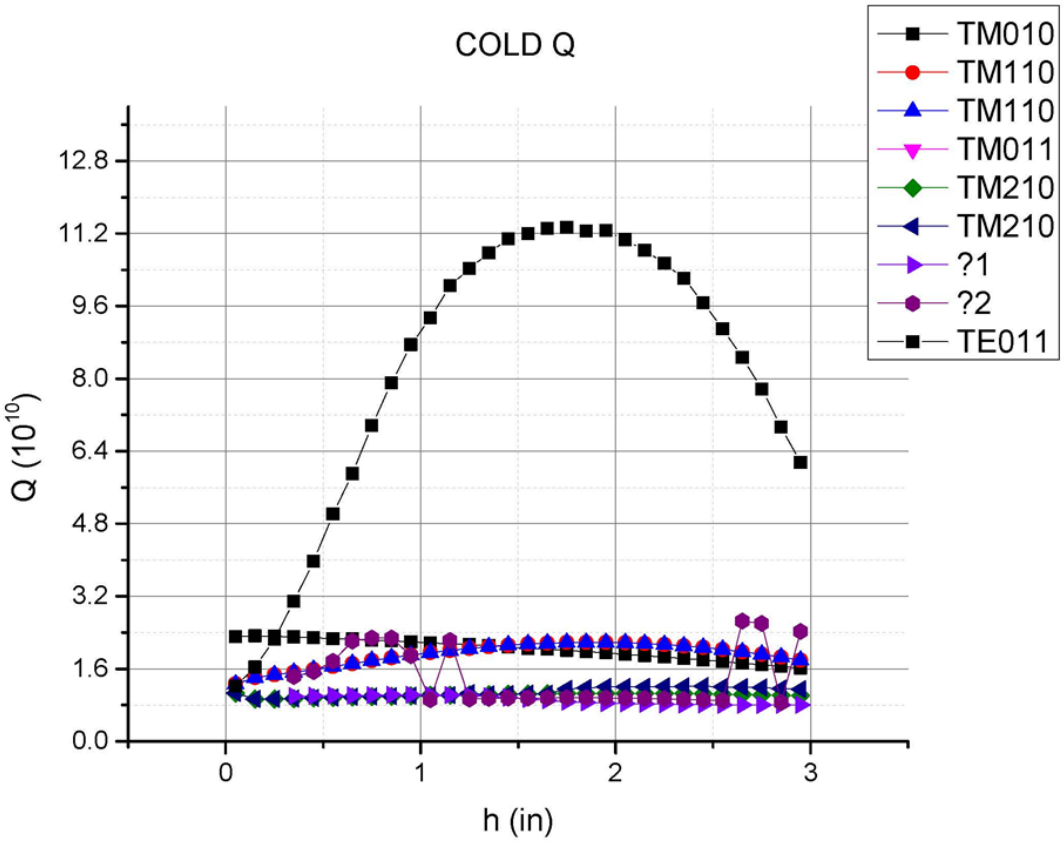

Figure 13: Plot of the Quality Factor (in units of 10^{10}) Versus the Height of the Crystal Above the Sample Plate

The 3 dimensional models also served as the basis for the thermal modeling that was done to find what the true critical field that could be achieved was. After running the parametric model through the varying crystal heights, it was found that the highest ratio of surface magnetic field on the sample versus the surface magnetic field on the walls

was 9.02 to 1. Other information that was necessary was the ratio of energy stored in the sapphire versus total stored energy in the cavity.

$$Q_0 = \frac{\omega U}{P}$$

Equation 1

$$U = \frac{\mu_0}{2} \int H^2 dV$$

Equation 2

$$P_{cavity} = \frac{R_s}{2} \int H^2 dS$$

Equation 3

$$P_{Sapphire} = \omega tan\delta E_{die}$$

Equation 4

The above equations illustrate the values that need to be derived from the numerical modeling in order to simulate the maximum fields in the cavity. H is the magnetic field, μ_0 is the permeability of free space, R_s is the surface resistance of the niobium, and tanδ is the loss tangent of the crystal and it is a function of temperature. Equation 1 gives the quality factor which is a ratio of the stored energy to the power lost in the cavity, scaled by the frequency. Equation 2, Equation 3, and Equation 4 give the method that the quantities in Q_0 are calculated. The integrals are taken numerically within Comsol and with some simple relations we can derive some very useful data about the wafer test cavity.

II.V. Mathematica Numerical Modeling

A numerical model was developed and coded into Mathematica to predict the maximum RF magnetic field that could be put onto a sample material in the wafer test cavity. The maximum magnetic field is determined by the losses in the sapphire and the properties of the cavity. From previous and current simulations it was found that a maximum occurs and then equilibrium is reached that is considerably lower than the maximum achievable field. This means that in order to get maximum performance and data from the cavity, it needs to be pulsed and allowed to cool before another pulse is introduced. For this reason the cooling of the sapphire was also simulated to give the repetition rate that can be utilized, while maintaining maximum performance of the cavity.

II.V.I. Model Development

This model was developed in the design work performed on the cavity in [11], by A. Sattarov and solved using a 4^{th} order Runge Kutta method [22]. The following derivation follows from the work performed in the above references and has been adapted to updated information on the cavity and loss tangent of the sapphire crystal obtained from Crystal Systems. First it is assumed that the thermal conductivity and the heat capacity can be treated with a cubic dependence on temperature as shown in Equation 5 and Equation 6.

$$\kappa(T) = \kappa_0 T^3$$

Equation 5

$$C(T) = M_s c_0 T^3$$

Equation 6

We can then write the electromagnetic energy of the cavity and thermal energy of the crystal.

$$\dot{E_{em}} = -\frac{\omega E_{em}}{Q(T, tan\delta)} + P_0$$

Equation 7

$$E_{thermal} = \int_{T_b}^{T} C(T)dT = \frac{1}{4} M_s c_0 (T^4 - T_b^4)$$

Equation 8

$$\dot{E}_{thermal\ out} = \frac{A}{L}\int_{T_b}^{T} \kappa(T)dT = \frac{A\kappa_0}{4L}(T^4 - T_b^4) = \frac{A\kappa_0}{Lc_0} E_{thermal}$$

Equation 9

$$\dot{E}_{thermal\ in} = \omega tan\delta\sigma E_{em}$$

Equation 10

Equation 7, Equation 9, and Equation 10 represent the time rate of changes of the energy in the cavity. Equation 7 gives the power input P_0 and subtracts the power lost to the crystal and the cavity surface. Equation 9 represents the power removed due to heat conduction of the crystal to the thermal bath. Equation 10 is the heat absorbed by the crystal due to the loss tangent of the sapphire. And finally Equation 8 is the thermal energy of the sapphire. The following relations can be combined to form a system of

ordinary differential equations that can be solved and used to derive the desired values of the cavity.

$$\dot{E_{thermal}} = \omega tan\delta\sigma E_{em} - \frac{A\kappa_0}{Lc_0} E_{thermal}$$

Equation 11

Equation 7 and Equation 11 will be solved simultaneously using the numerical differential equations solver in Mathematica, subject to the boundary conditions that the thermal and electromagnetic energy in the cavity are initially 0. The Mathematica code is included in Appendix A, with the constants values and definitions included. The entire code with the cooling term and pulse length are included, which is illustrated in Equation 12.

$$\left\{ \begin{array}{ll} \dot{E_{em}} = -\frac{\omega E_{em}}{Q(T, tan\delta)} + P_0, & t \leq t_0 \\ \dot{E_{em}} = -\frac{\omega E_{em}}{Q(T, tan\delta)}, & t > t_0 \end{array} \right\}$$

Equation 12

II.V.II. Modeling Results

Two situations were modeled for the test cavity; the first is assuming that the power is continuous wave (CW) and the second that the power is pulsed. The CW case was compared to previous models and a hand calculation, evaluated using an excel spreadsheet. The cavity energy, magnetic field and sapphire temperature are evaluated.

II.V.III. CW Model Results

The CW power model gives the highest theoretical magnetic field achievable in the cavity, which is 162 mT or 81% of the critical RF magnetic field of niobium, which is shown in Figure 14. The values of the Quality factor are normalized to the values that were derived from the wafer test cavity measurements at TJNAF and the loss tangent used was from a 7^{th} order fitting function from [11]. The measurements of the wafer test cavity confirmed the values found in the above reference, for the loss tangent. If the loss tangent could be lowered by a factor of 2, the maximum magnetic field on the sample would be raised to 201 mT, giving the BCS critical RF magnetic field on the sample material. The energy of the cavity and temperature of the sapphire are plotted in Figure 15 and Figure 16, respectively.

II.V.IV. Pulsed and Cooled Model Results

The next step in the modeling progression was to evaluate the cavities performance when the power is pulsed and the sapphire is cooled from the contact with the thermal bath of the dewar. This information will give the pulse length necessary to achieve the maximum magnetic field and the time it takes for the sapphire to cool, before it can be pulsed again. The time that it takes to reach the maximum magnetic field can be roughly derived from the previous sections plots, which is a 2 ms pulse length. This time gives the maximum magnetic field, while avoiding unnecessarily heating the sapphire. The characteristic time constant for the sapphire to cool is shown in Equation 13. Using the values for the wafer test cavity we get a time constant of 25.6 ms.

$$\tau_{cooling} = \frac{LM_s c_0}{\kappa_0 A} = 25.6\, ms$$

Equation 13

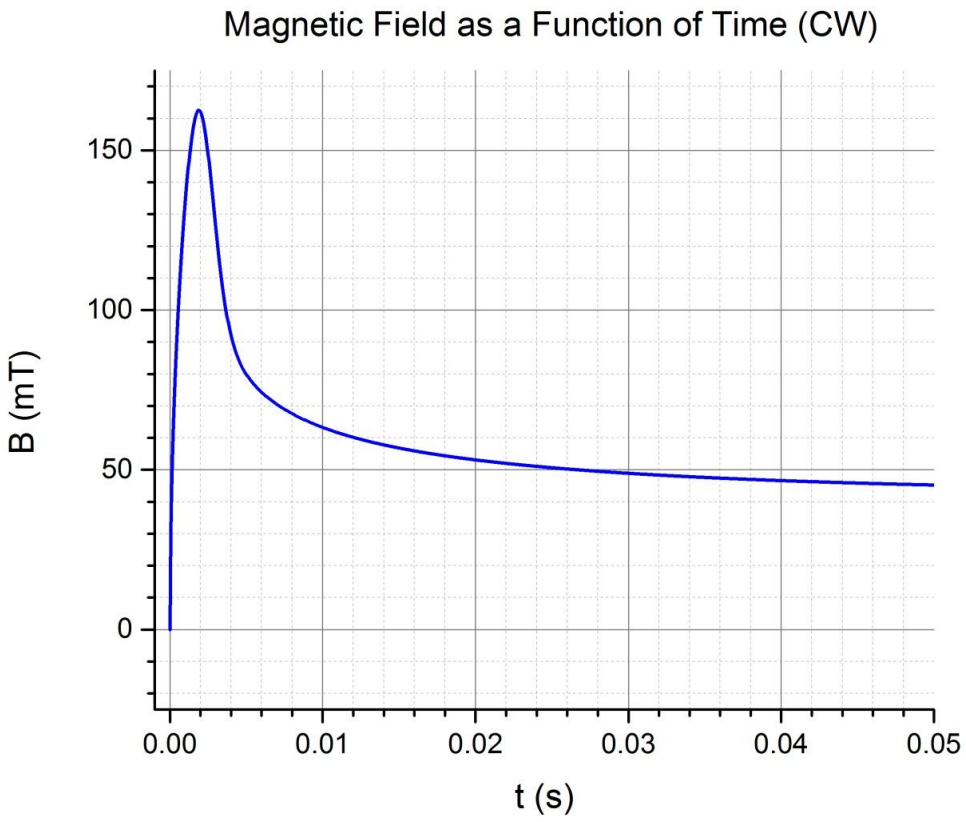

Figure 14: Magnetic Field of the Wafer Test Cavity with 500 Watts of Continuous Power

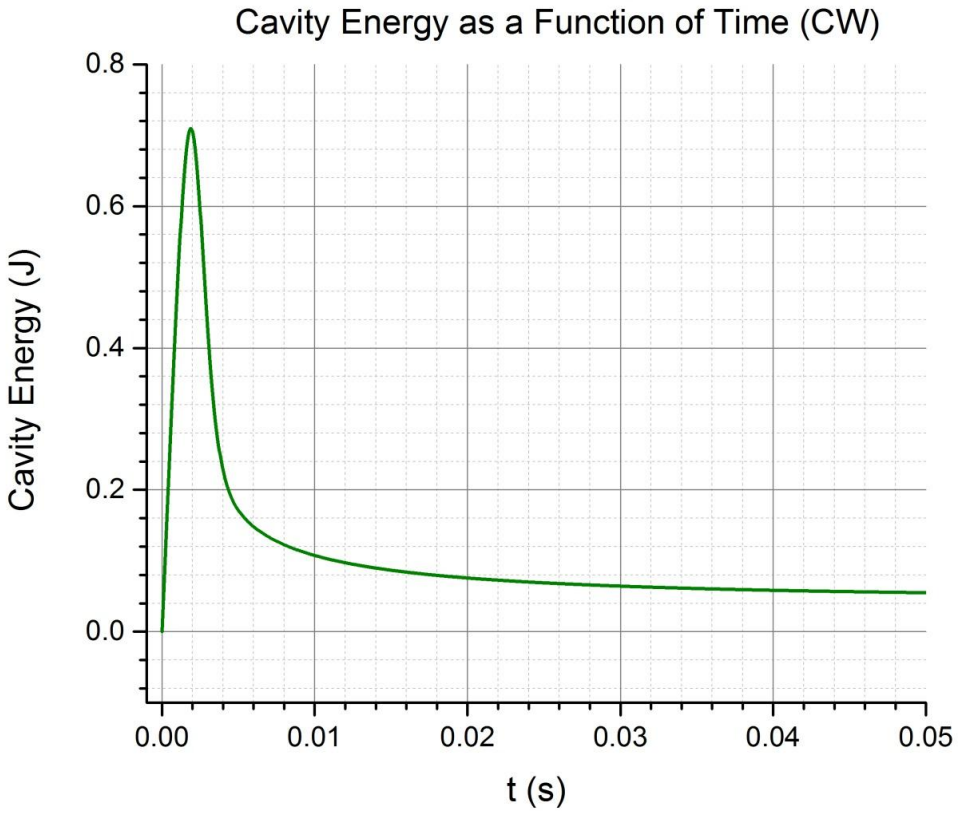

Figure 15: Energy of the Wafer Test Cavity with 500 Watts of Continuous Power

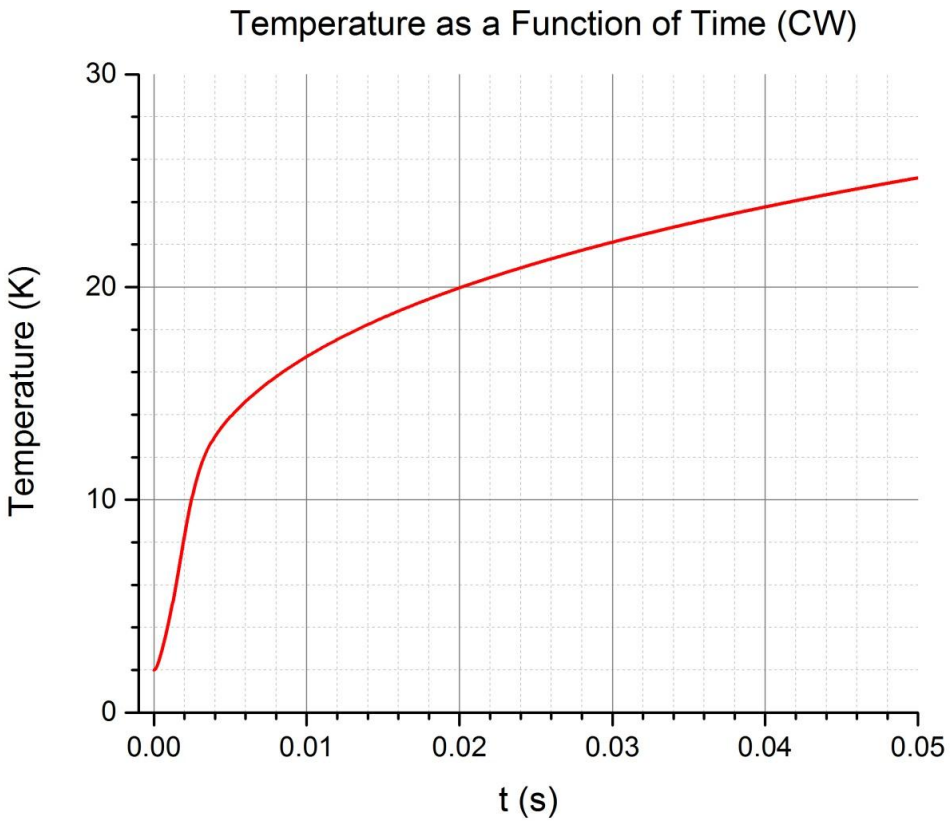

Figure 16: Temperature of the Sapphire with 500 Watts of Continuous Power

The results from running the simulation with a 500 W, 2 ms pulse gives the desired magnetic field in the cavity, as shown in Figure 17. The cooling time necessary for the sapphire to reach a temperature where it can be pulsed again is several time constants in length. Figure 18 shows that a time of 200 ms is necessary before the crystal is returned to a level that the cavity can be pulsed again.

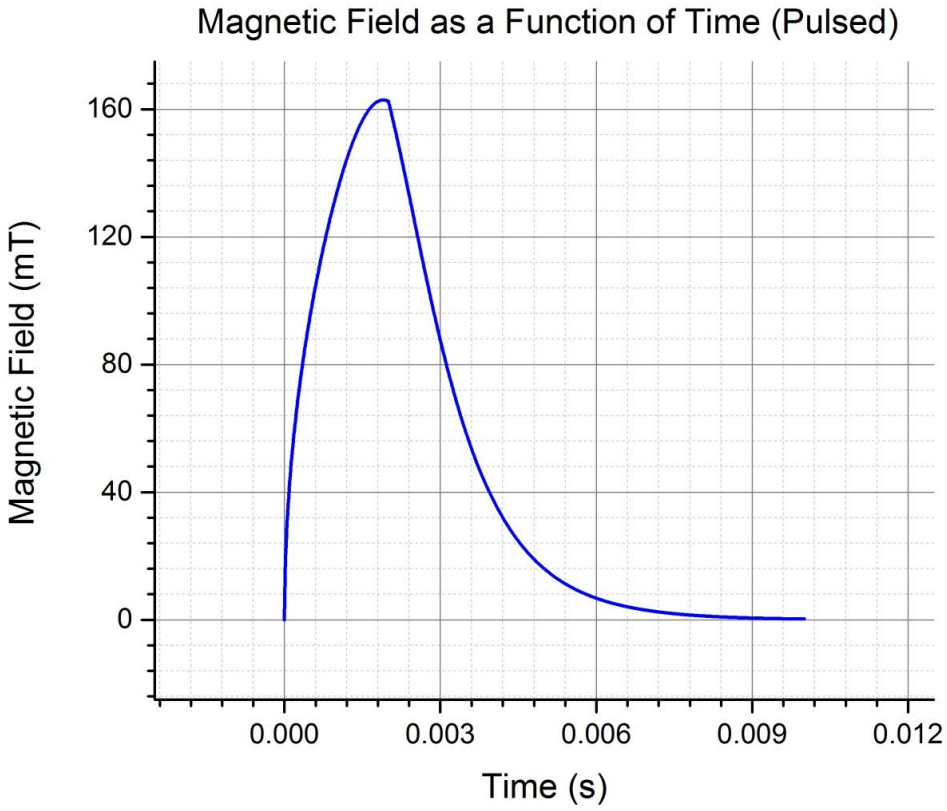

Figure 17: Magnetic Field of the Wafer Test Cavity with 500 Watts of Pulsed Power

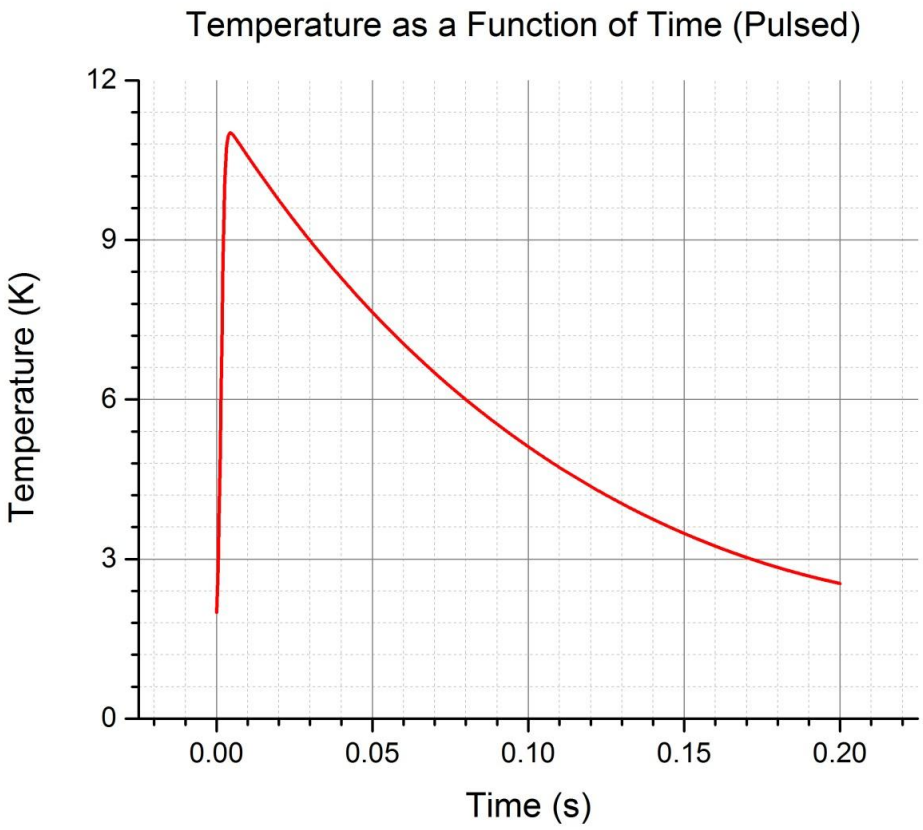

Figure 18: Temperature of the Sapphire with 500 Watts of Pulsed Power

III. EXPERIMENTAL SETUP

III.I. Cavity Construction

The fabrication of the cavities main components was performed by Larry Turlington at TJNAF, Figure 19 shows the main body of the cavity. This was done to the specifications set by the scientist and researchers at Texas A&M University. The cavities overall design and construction was performed prior to the beginning of the work presented in this thesis, so the focus will be on the work done after the main components were constructed.

Several components had to be manufactured before testing on the cavity could begin, these included feed-throughs for couplers and vacuum equipment. A replacement for the sample holder and sample material was made to simplify the assembly and testing for this work. A plate of 3/8" RRR niobium was used to fabricate a 7.024" diameter base plate for the cavity. This was done to prevent unnecessary deflection due to pressure differences between the cavity and dewar. A length of 316L stainless steel tubing, 316LN mini-conflat flanges and custom feed through flanges for the cavity were acquired for the fabrication of the feed-throughs. The custom flanges were machined by the main TJNAF machine shop. An issue that arose was that the tubes that were cut for the feed through were welded together, the order was incorrect. Instead of getting a long straight section of tube for the RF coupler to be placed in, two shorter sections were used. This caused the tube to be bent and caused issues later on with coupler placement

and possible issues with coupler discharges. A picture of the 4 way cross is shown in Figure 20, with the associated equipment attached.

Figure 19: Completed Body Section of the Wafer Test Cavity with Niobium Main Components and NbTi Flanges

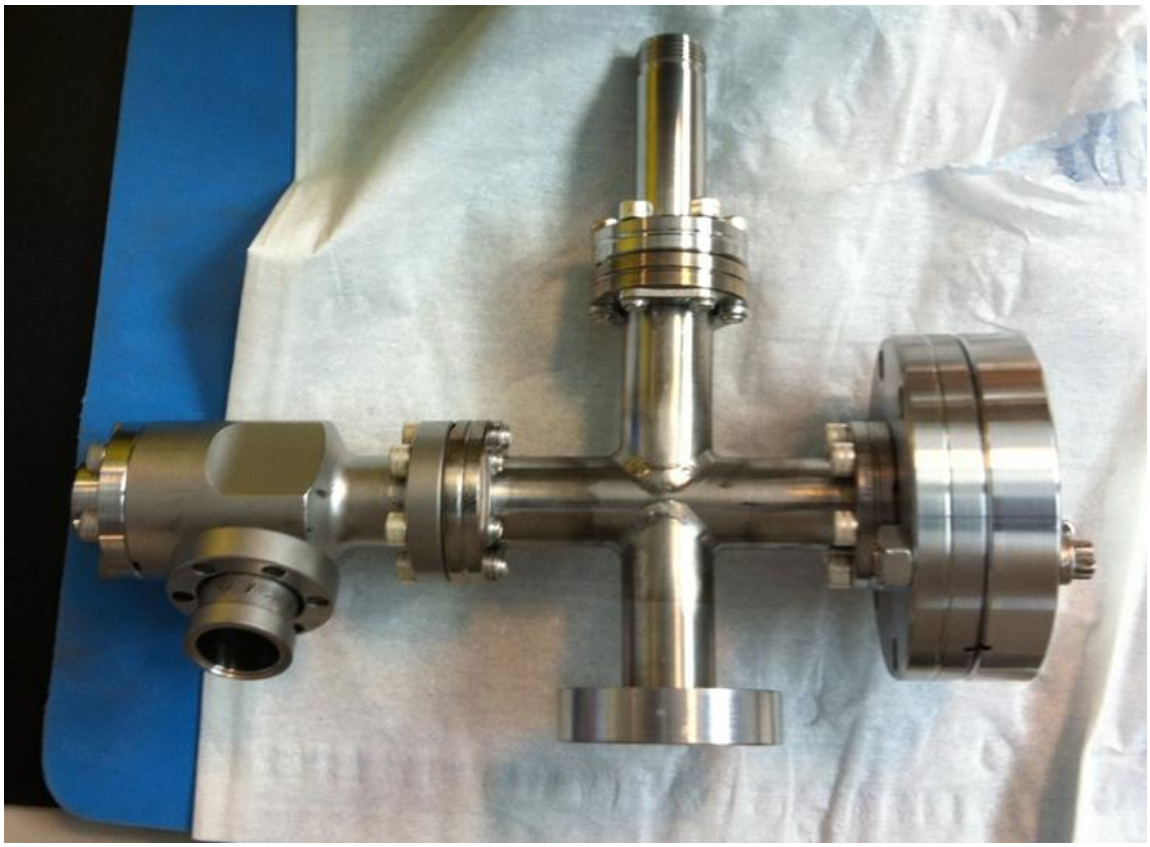

Figure 20: 4 Way Adapter With Vacuum Valve (Left Arm), Type-N RF Feed-Through (Top), Space For Blow Out Disc (Right Arm) and Cavity Flange (Bottom)

The main issue with machining of the components for the cavity was the use of 304 stainless steel, because it was found to have a relative permeability of greater than 1.1, in certain places. This issue was deemed to be insignificant due to the time constraints of this project and it's placement in a low field region of the cavity. Another issue with the stainless steels used, was the 316LN from the TJNAF machine shop being just as high as the 304 stainless steel. Aside from these small issues, the cavity and all of its components were constructed in an efficient manner.

III.II. Bench Top Setup

For the bench top testing and coupler calibration the cavity was not cleaned or sealed. This is because it would have to be handled extensively to get the coupling correct and the mode structure mapped. The crystal was originally left out to avoid having any further complications to the process of mapping the modes. The outcome of this and the other testing will be described in the next section, so it will not be discussed here. Initial experimentation was done using a network analyzer and flanges designed to use welding wire as the antenna, pictured in Figure 21. This setup was later modified to use different couplers, but the experimental setup stayed essentially the same.

III.III. First Cold Test Setup

The first cold test was performed in Dewar 1 at TJNAF, because it is designated as a low power level Dewar and it was available at the time of testing. Since we were only using a network analyzer to find the mode at cryogenic temperatures and take rough Q measurements, this was quite acceptable. A picture of the cavity on the Dewar 1 test stand, being lowered into the Dewar, is shown in Figure 22. An Agilent Field Fox handheld network analyzer was used on Dewar 1, as it was available and more than capable for the test that was being performed.

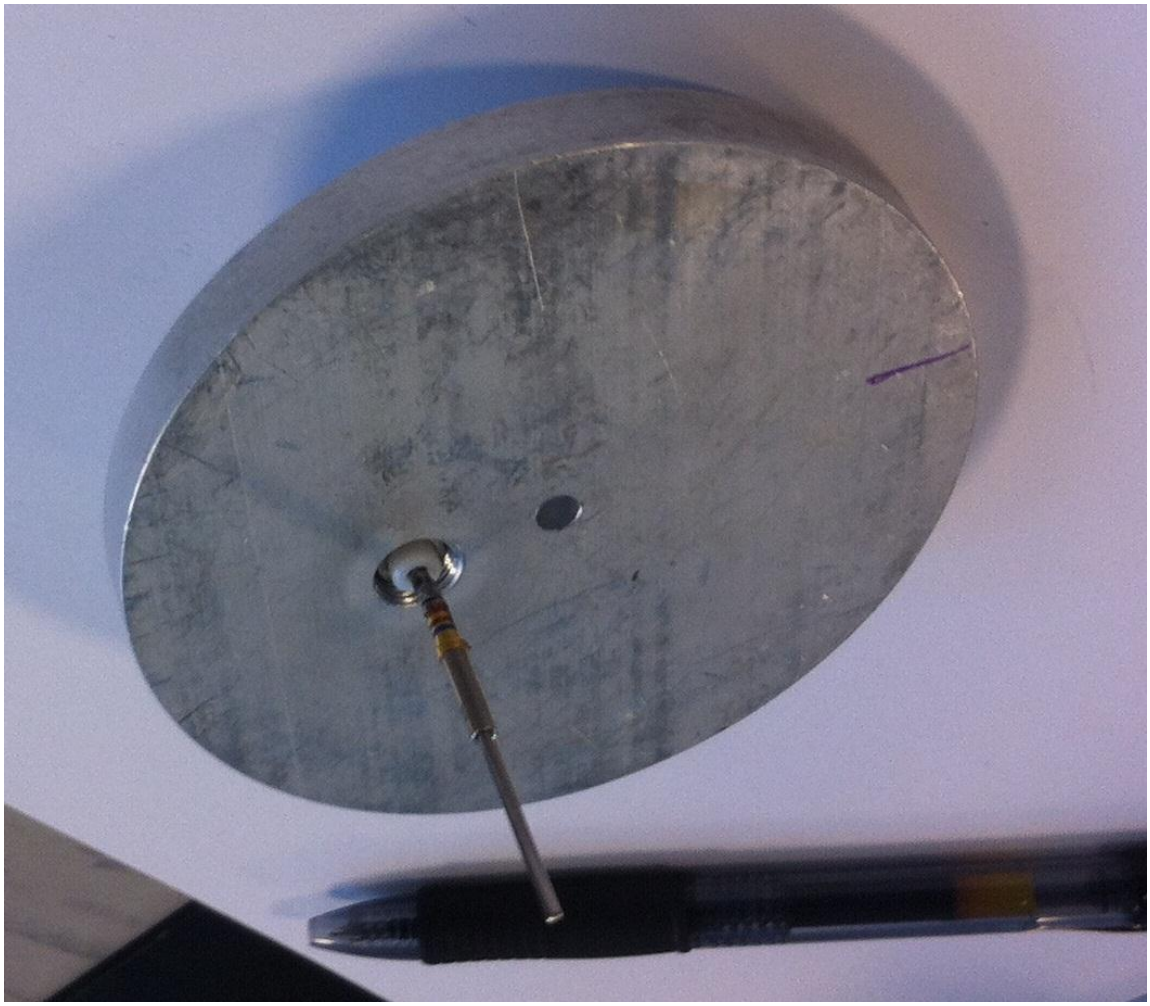

Figure 21: Aluminum Flange With Adapter For Using Welding Rod Antennas

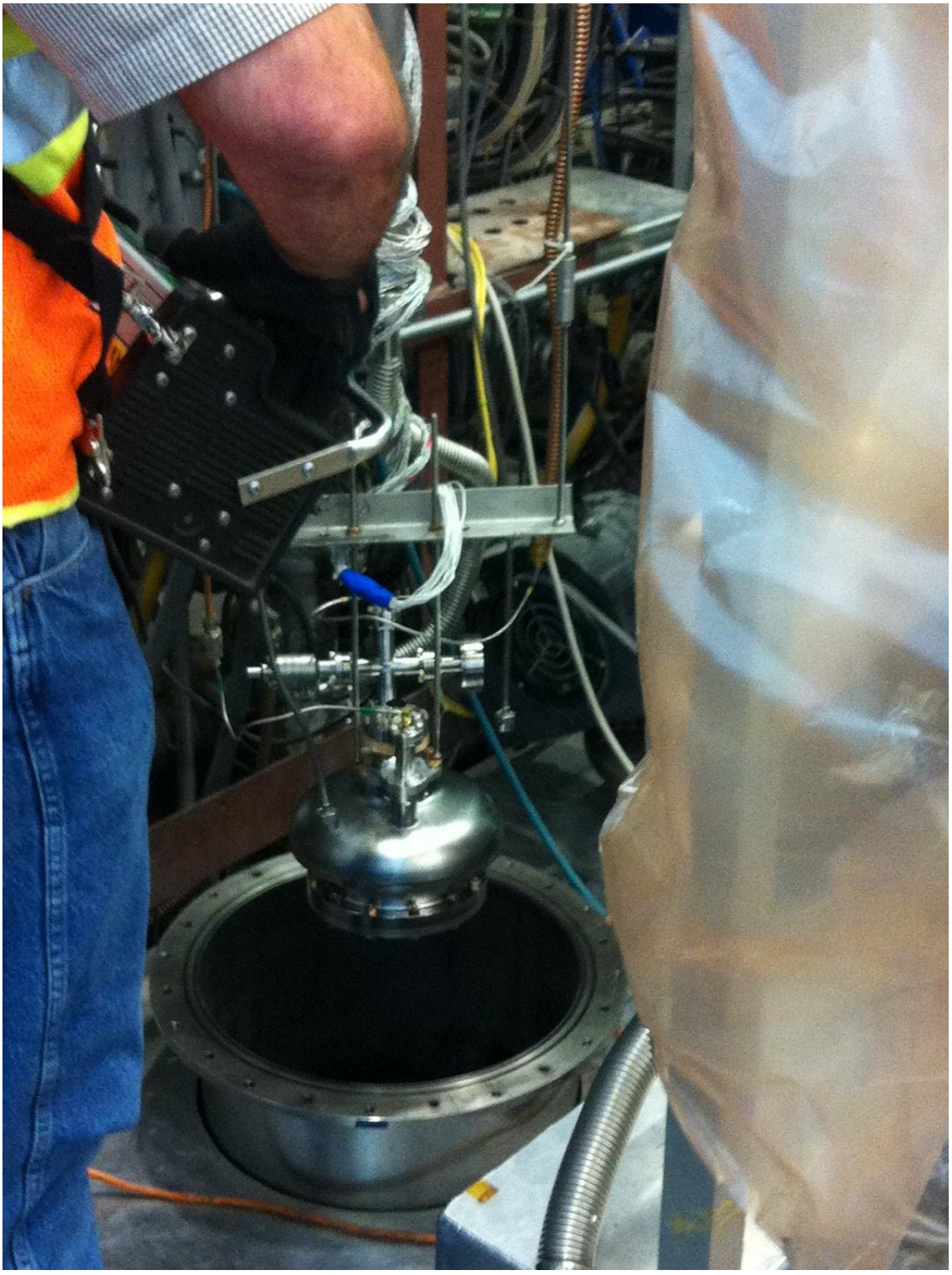

Figure 22: Dewar 1 Test Stand With Wafer Test Cavity Attached at the Base Being Lowered into Dewar

III.IV. Test 2, 3 and 4 Setup

The remaining 3 tests were performed on the larger, blast shield protected Dewars, using a network analyzer and the research and development phase locked loop (PLL) RF system. The main issue with testing using the PLL system was finding RF components in the frequency range that was required. The frequency was too high to use the standard RF amplifiers employed by TJNAF. A Keltec SR630-200 2.0-4.0 GHz amplifier was sourced to be used for the testing of the wafer test cavity. After a short test of the gain of the amplifier it was determined that it had sufficient bandwidth to cover the 1.87 GHz that was necessary. A circulator was difficult to find in the frequency range necessary, but a UTE CT-2103 circulator was found to be effective 1.0-2.0 GHz, Figure 23 shows the circulator used. The final component that had to be found was a directional coupler and a suitable Narda model 3022 Bi-Directional coupler was found that had a range of 1.0-4.0 GHz, Figure 24 shows the directional coupler used.

The phase locked loop RF system design is beyond the scope of this thesis, but a comprehensive document has been written by Tom Powers of TJNAF [23]. The particular RF system used for the testing of the Wafer Test Cavity was the research RF system, as it was the only system that was in the frequency range necessary.

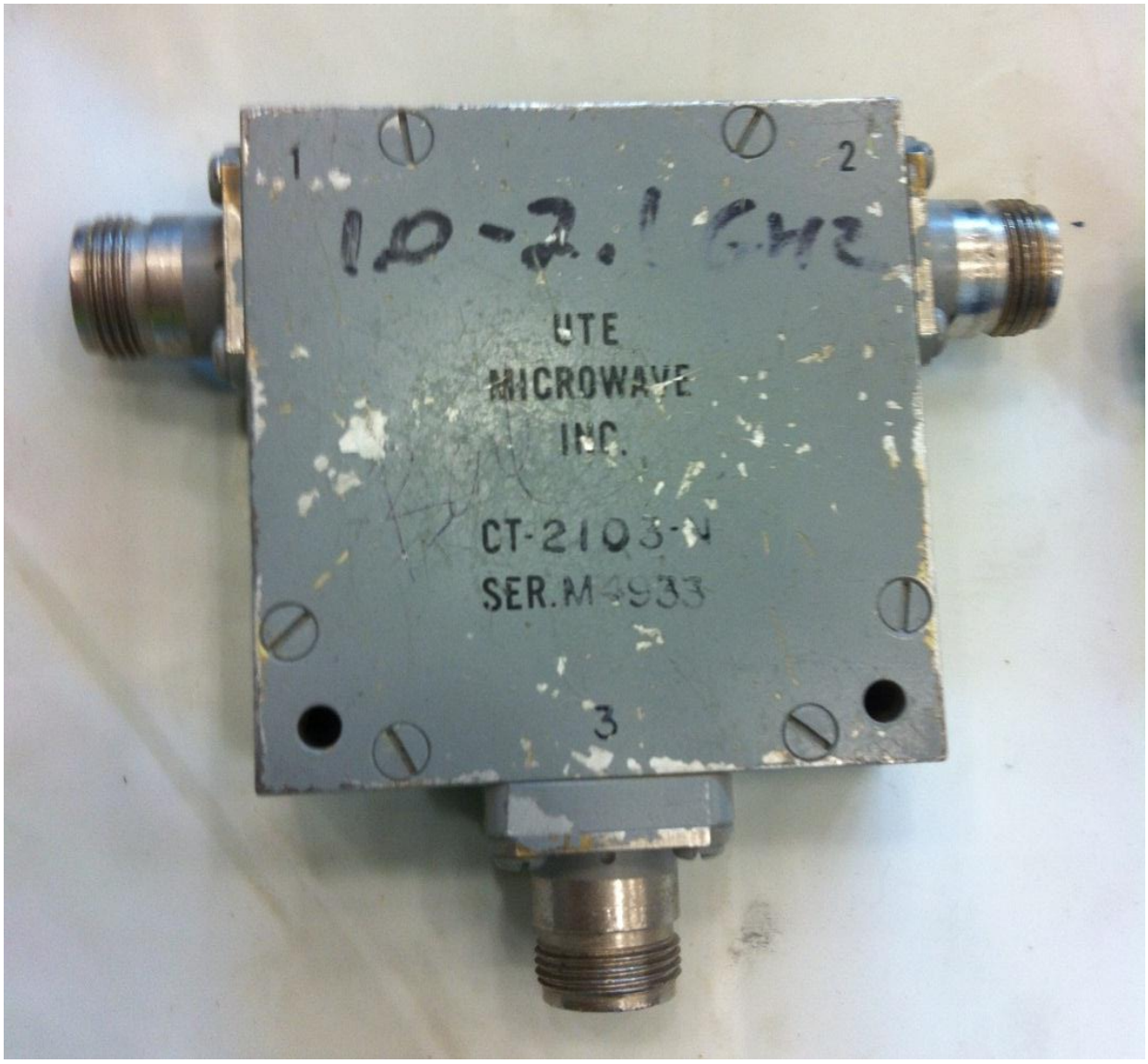

Figure 23: UTE Microwave Inc. CT-2103 Circulator

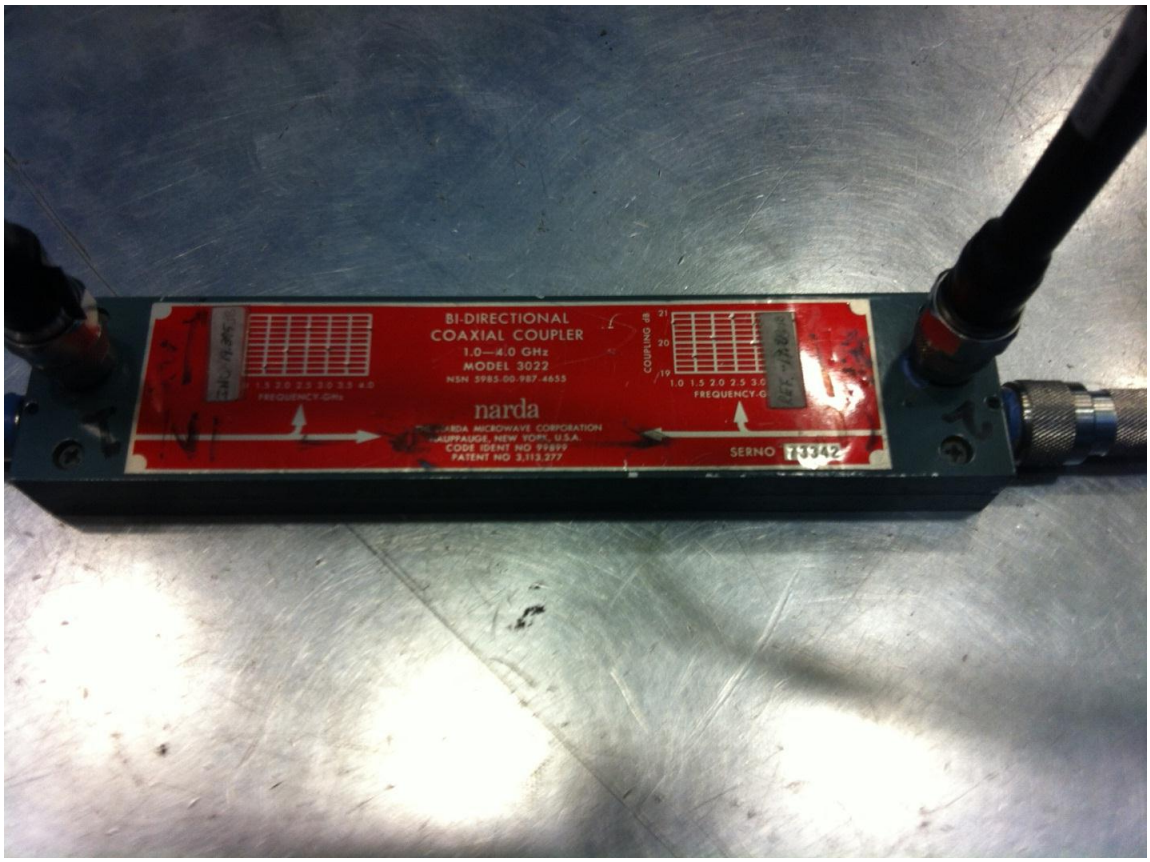

Figure 24: Narda Bi-Directional Coaxial Coupler Model 3022

III.IV.I. Sapphire Cleaning Procedure

The sapphire preparation was pointed out as a significant issue by Dr. Pogue, prior to the testing performed in this work. For this reason, special care was taken to prepare the sapphire and to store it prior to cavity assembly. The procedure used was sourced from [11, 16], which are adaptions of the procedure used by NASA Jet propulsion Laboratory [24]. The procedure used was to create a nitric acid solution with: one part pure nitric acid, three parts water. Then place the sapphire in the solution and

perform an ultrasonic cleaning for 5 minutes. After ultrasonic cleaning, the solution was heated until it began to boil, and then allowed to cool to room temperature. After 20 minutes of cooling, the sapphire was removed from the nitric acid and washed with D.I. water. The sapphire is then placed in a beaker with acetone and ultrasonically cleaned for 5 minutes, rinsed in isopropanol and placed in a beaker of isopropanol and ultrasonically cleaned for 5 minutes. The sapphire is finally placed in ethanol and ultrasonically cleaned for 5 minutes. The sapphire is then left in the ethanol until assembly of the cavity. It is also important that the time the sapphire is out of alcohol or vacuum is minimized to maximize the performance of the cavity.

III.IV.II. Cavity Cleaning Process

The cavity was prepared in the same manner for all 4 cold tests, which included a Buffer Chemical Polish (BCP), followed by an ultrasonic bath cleaning using Micro-90 detergent and rinsing in 18 MΩ deionized water. BCP is a mixutre of hydrouoric acid, nitric acid, and phosphoric acid in a 1:1:1 ratio. The first BCP was performed in the BCP cabinent in the clean room. Chemistry hardware was designed and constructed to allow the cavity to be conntected to the BCP cabinents hoses. A picture of the cavity, on the BCP test stand, in the BCP cabinent, is presented in Figure 25. The remaining BCP processes were performed by hand by qualified technicians, which included Teena Harris, Jim Follkie and Era Perry. The first BCP was a 100 μm procedure, where 100 μm was removed from the cavities internal surface. Once the parts were cleaned they were placed in anti-static plastic bags, filled with dry nitrogen and sealed. The cleaned

parts were then placed in a pass through so that they can be brought into the clean room. The cavity can then be assembled in TJNAF's class 10 cleanroom.

III.IV.III. Cavity Assembly

The cavity was cleaned again with dry nitrogen over a particulate size detector and placed on a cart. Pre-assembly was made of all the Conflat parts to limit the amount of work after the indium seals were finished. The indium is then sprayed with acetone on a clean surface and rolled in the acetone bath. The indium is then pulled through an acetone soaked rag and placed to the side. After all the necessary pieces are cleaned, the same process is repeated with isopropyl alcohol to remove any acetone residue. The order of assembly for the cavity was important to ensure that the indium seals stayed intact. The cavity was designed with a notch in the bottom NbTi ring, which was sized to accept a 0.06" indium wire to simplify the assembly of the cavity. This feature was not used as it would make cleaning very difficult with indium stuck in a small inaccessible groove. Instead a 0.04" indium wire was placed on the outside edge between the groove and the outer bolt pattern, Figure 26 shows the layout of the base mounting plate. The main source of problems for assembly and ultimately the vacuum achievable was determined by the quality of this bottom seal. The assembly of the cavity began with the placement of the crystals height and then its seal to the top indium seal flanges. The crystal was placed on top of a 0.5" gauge block, set on top of the bottom 3/8" niobium plate. Then 0.04" indium was wrapped around the crystal into the groove provided. The top plate was placed over the indium wire and crystal and was bolted down using silver-coated screws.

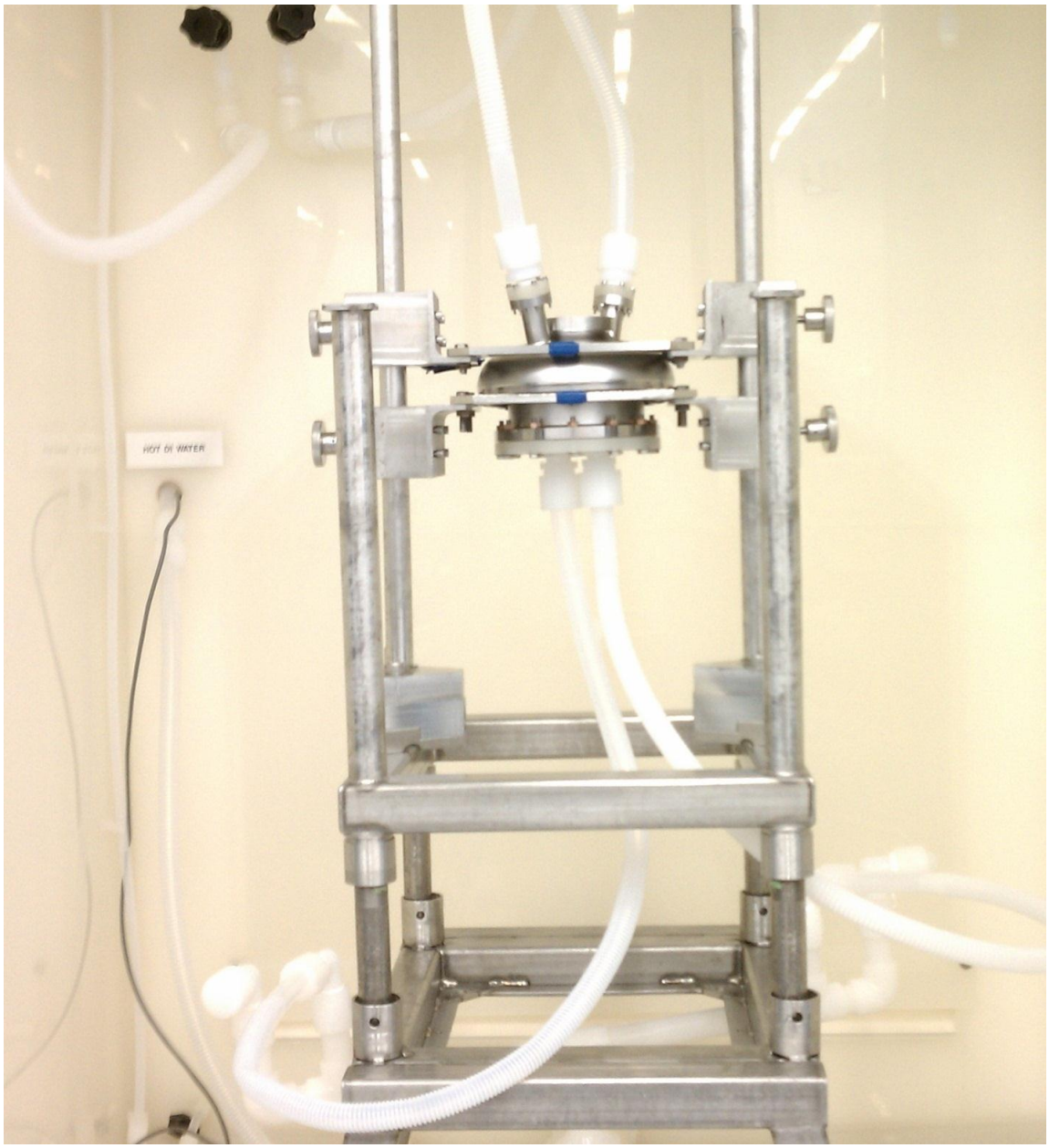

Figure 25: Wafer Test Cavity in the BCP Cabinent Connected Via Custom Chemistry Flanges

A torque wrench was used in progressively higher torques to ensure uniform tightening of all indium seals. Once the crystal was in place the gauge block was

removed and the cavity was flipped on its top and supported, as to not disturb the crystal. The base plate indium seal was carefully placed and the bottom plate was bolted using the same torque wrench method. Finally the coupler assemblies were bolted the coupler NbTi flanges by placing a circle of indium wire on them and carefully torqueing the fittings down.

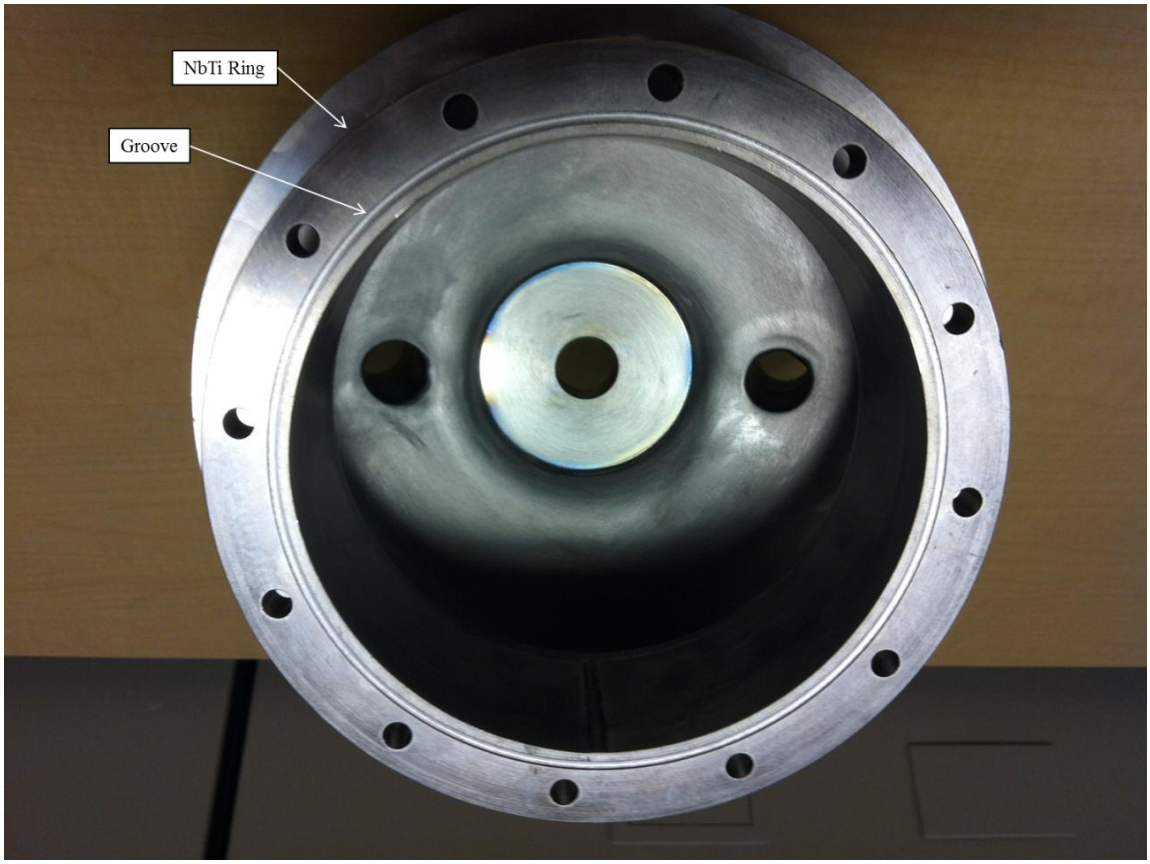

Figure 26: Schematic Showing the Indium Wire Groove and NbTi Base Plate Ring

IV. EXPERIMENTAL RESULTS

IV.I. Bench Top RF Measurements and Coupler Fabrication

Bench top measurements were made on the test bench in the test lab addition (TLA) in the RF structures room. A 5071C Agilent network analyzer was used to measure the mode structure and set the Q_{ext} for the incident and transmitted antennas. The original couplers used were straight rod couplers, attached to type-n feed-through's. These couplers do not couple well to the TE_{011} mode and after a short effort; a switch was made to hook type couplers. Hook type couplers did not offer the improvement that was expected when coupling to an electric field. While the mode could be found, it was weak and it was decided that loop couplers would be more beneficial for the first test to find the mode at cryogenic temperatures. Figure 27 shows the straight and hook coupler mode structures, while some improvement was made, it was not appreciable.

Several issues were addressed after this initial investigation. First the mode structure was better simulated to find the best position to set the crystal to find the TE_{011} mode. Second, loop couplers were made from semi-rigid coaxial line and sma-sma feed-throughs, pictured in Figure 29. The results of changing to loop type couplers can be seen in Figure 28, where there is considerable mode separation and the TE011 mode is at 1.872703125 GHz. The input Q_{ext} was set at $5x10^7$ and the output at $3x10^9$.

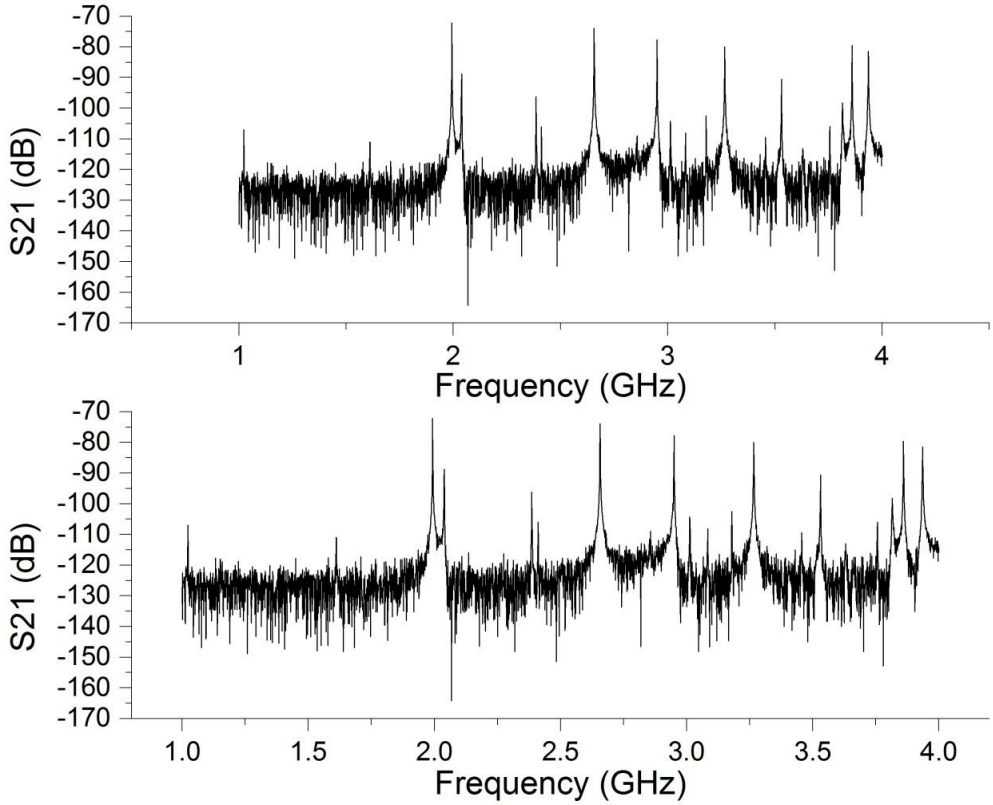

Figure 27: Straight (bottom) and Hook (top) Mode Structures, Where the TE011 Mode is at 2.15 GHz for the Unloaded Cavity

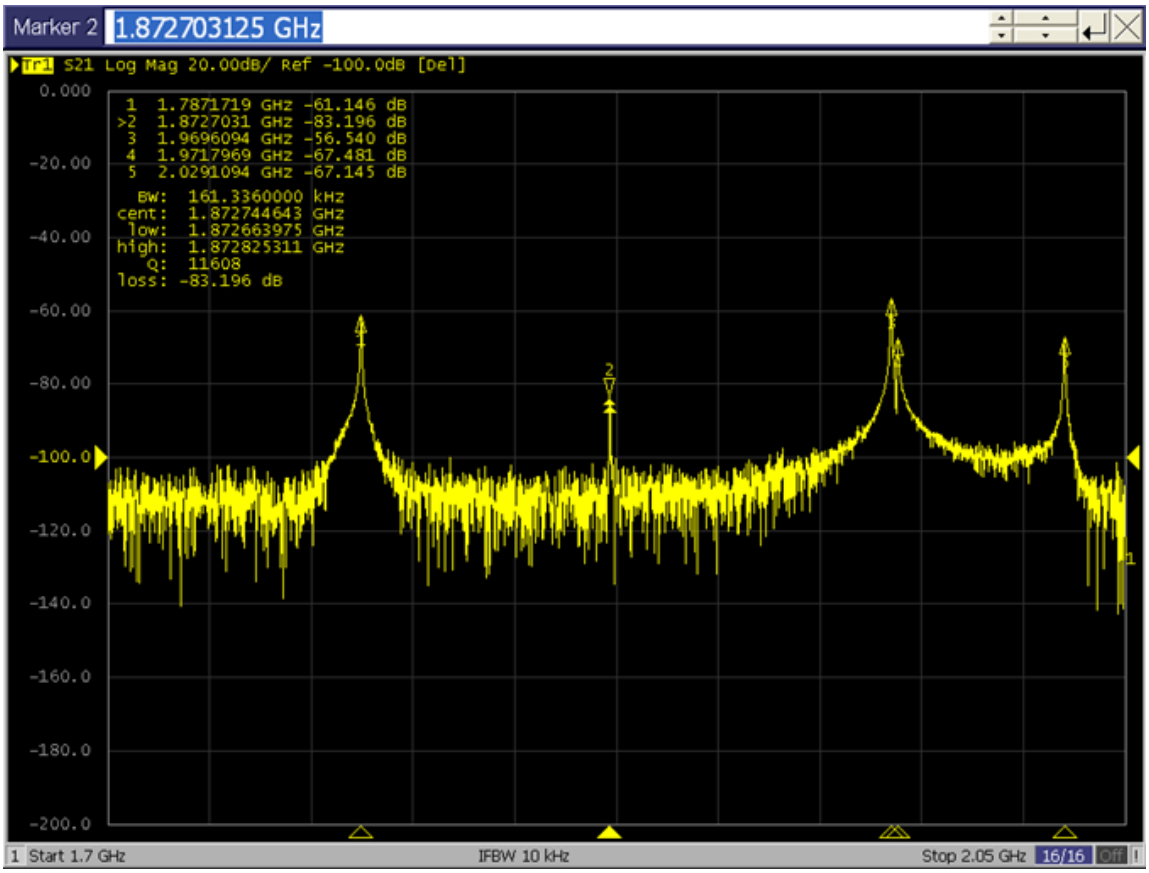

Figure 28: Mode Strucutre From 1 to 2 GHz, With TE_{011} Mode at 1.8727 GHz

Figure 29: Loop Couplers Made From Semi-Rigid Coaxial Line and SMA to SMA Vacuum Feed-Throughs

IV.II. First Cold Test

The first cold test was performed in Dewar 1 to find the frequency of the TE_{011}, check the coupling, and get a rough Q_0 measurement. The temperature of the bottom diode on the Dewar reported temperatures below 0 K, so the data should only be used for qualitative observations. At the time of the testing it was determined that the Q_0 was higher than the network analyzer could resolve, so that another test needed to be performed. This test also provided an opportunity to track the frequency and quality factor of the cavity as a function of temperature. Figure 30 shows the frequency as a function of temperature, where it should be noted that the calibration was off so the temperature is scaled down by approximately 2 K. An interesting feature of this plot is the frequency going down at a certain temperature. It is believed that this is roughly 4 K, as a vacuum must be pulled to get temperatures below that of liquid helium.

The quality factor as a function of temperature plot is presented in Figure 31 and it would appear that it lacks much in the way of features. At the time of testing this was a good sign as the network analyzer cannot resolve quality factors above approximately 10^7 so this meant that we had a quality factor high enough to require the use of the research RF system.

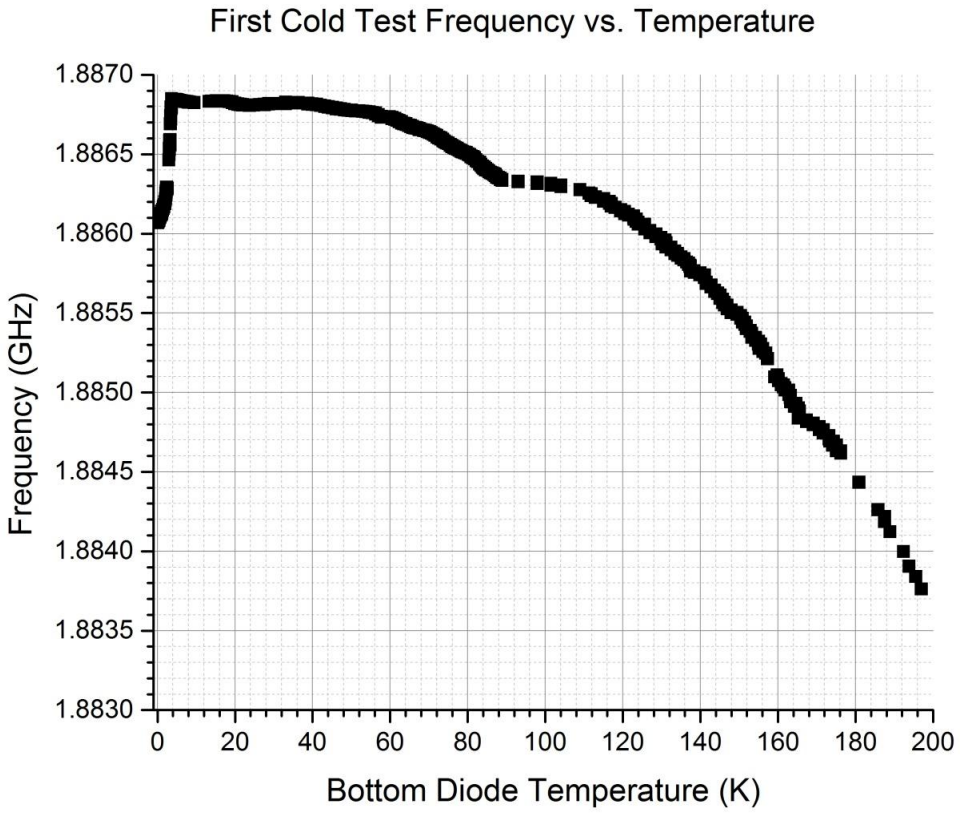

Figure 30: Frequency of the TE011 Mode versus Bottom Diode Temperature

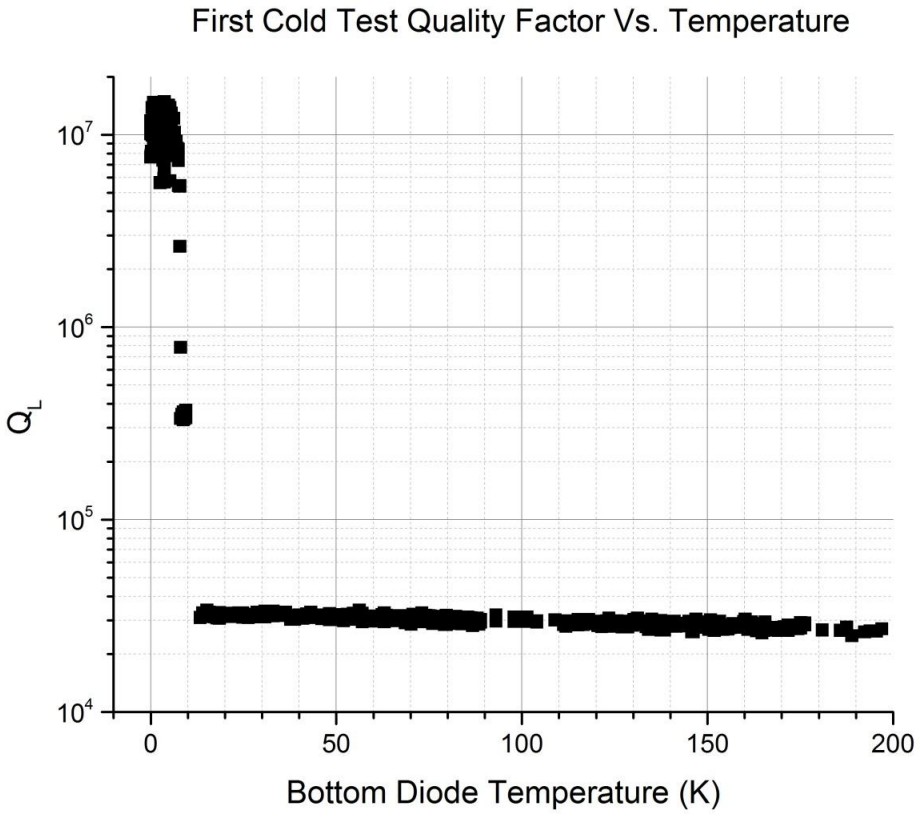

Figure 31: Loaded Quality Factor versus Bottom Diode Temperature

Overall the first test was a success as we got the cavity assembled and liquid helium tight. The cavities fundamental mode was found and tracked from 200 K down to 2 K and a quality factor measurement revealed that we had sufficient performance to warrant further testing of the cavity.

IV.III. Second Cold Test

The second cold test of the wafer test cavity was performed in two parts; first the cavity was cooled to 5 K and monitored with a network analyzer. At 5 K the cavity was

then switched over to the R&D RF system and was monitored from 4.23 K to 2 K. The measurements from room temperature to 5 K were monitored via a computer, but the measurements with the RF system had to be taken by hand.

Preparation for this test was similar to the first test, except Lakeshore Cernox resistors were attached the cavities body and to the top of the sapphire crystal to monitor their temperatures during the test. It was unsure at the time if this would be effective, especially once the helium reached a superfluid state, for measuring the temperatures separately. This is because the power produced in the crystal is rather small compared to the thermal conductivity of the helium bath. The resistors were attached to the cavity and sapphire with a cryogenic varnish, as can be seen in Figure 32.

IV.III.I. Second Cold Test Room Temperature to 5K Testing

From room temperature to 5 K the frequency, loaded quality factor, temperature of the cavity, temperature of the sapphire, and resonant peak width of TE011 mode were measured on an Agilent 5071C network analyzer, via a Labview program provided by Ari Palczewski. During this portion of the cool down, the quality factor and frequency were recorded simultaneously with the use of the network analyzer and the Lakeshore temperature monitor. Plots of the frequency and quality factor versus the temperature sensor on the Dewar are shown in Figure 33 and Figure 34, respectively.

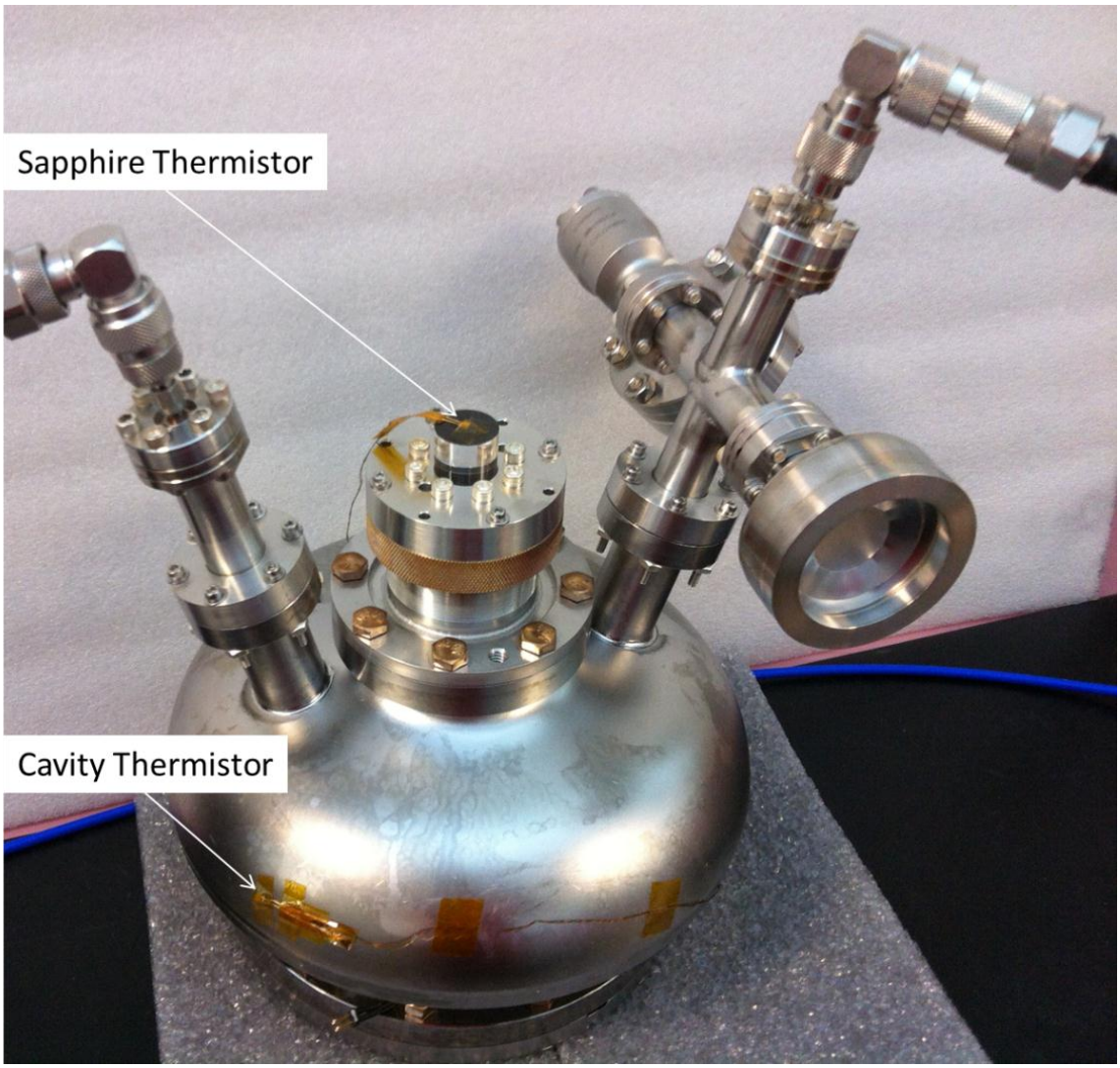

Figure 32: Assembled Cavity with Thermistor Layout

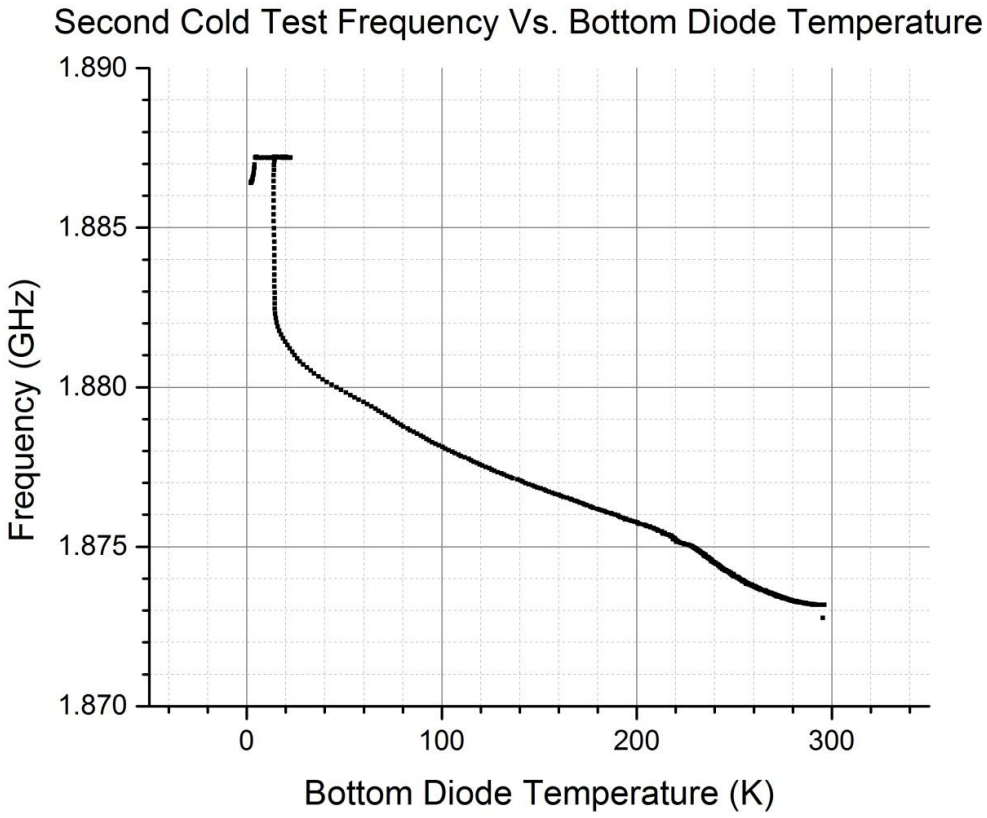

Figure 33: Frequency versus Temperature Room Temperature to 5K

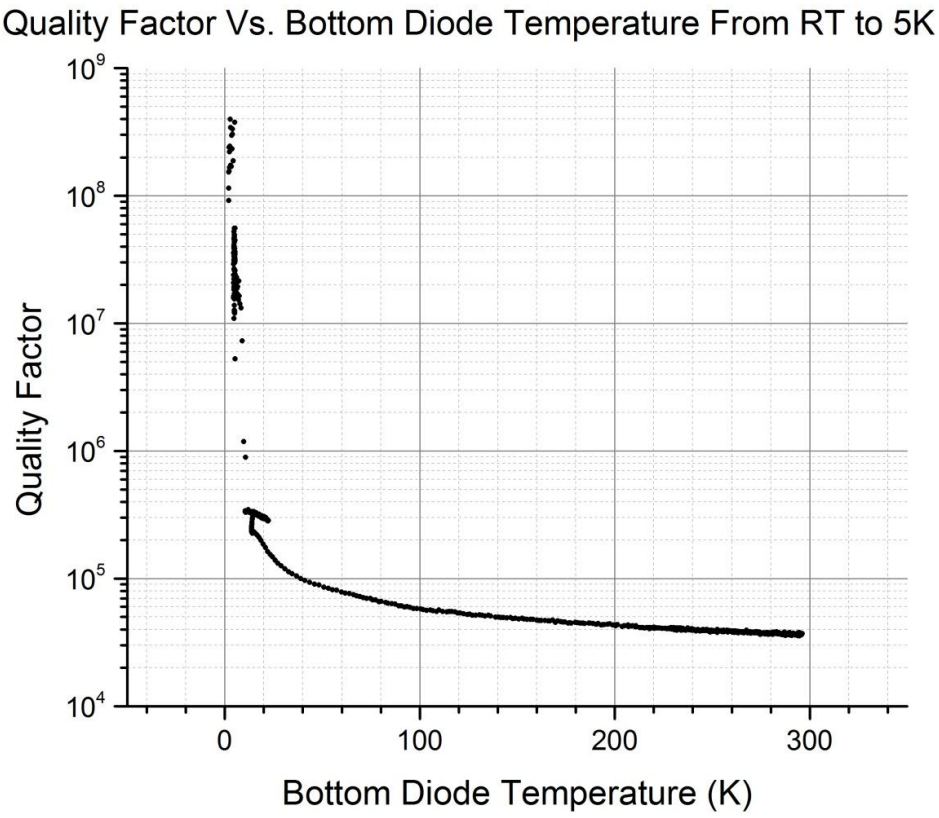

Figure 34: Quality Factor versus Dewar Temperature

The sapphire crystal cooled considerably slower than the cavity as a whole, the plot of the two separate temperatures is plotted versus time in Figure 35. There are two reasons for this, the cavity is cooled from the bottom and the crystal is only exposed on the top of the cavity and the crystal has a large thermal mass within the vacuum of the cavity with only a small portion being exposed to the cryogenic bath.

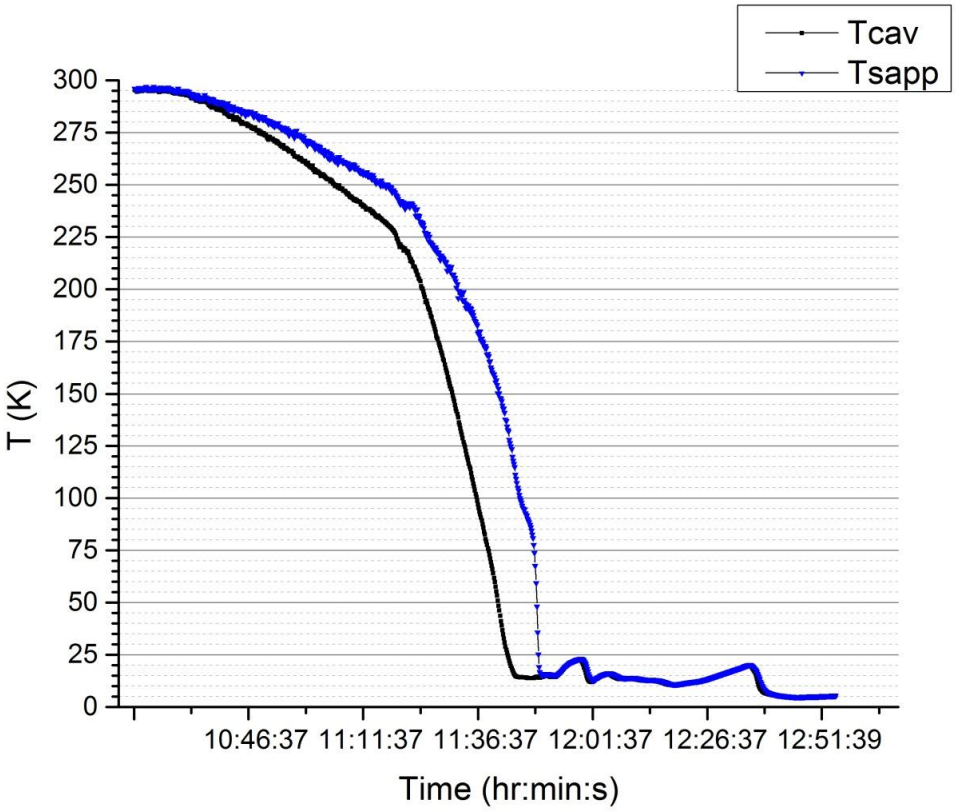

Figure 35: Cavity and Sapphire Temperature versus Cooling Time

IV.III.II. Second Cold Test 4.23 K to 2 K Testing

The RF test from 4 K to 2 K was performed by hand and entered into the standard spreadsheet used for RF testing in the VTA. For Q vs. T measurements, low-level RF was used from 4 to 2 K. It was very difficult to get a lock on the cavity with the PLL to take measurements. After a considerable amount of effort, Grigory Eremeev suggested adding an amplifier to the transmitted power. A 35 dB amplifier was added to the transmitted power output, but there was still considerable difficulty in getting a lock

on the cavity. The Frequency Modulation on the signal generator was then adjusted from 1 MHz to 10 MHz, which made locking the cavity much easier in conjunction with the amplified transmitted power line.

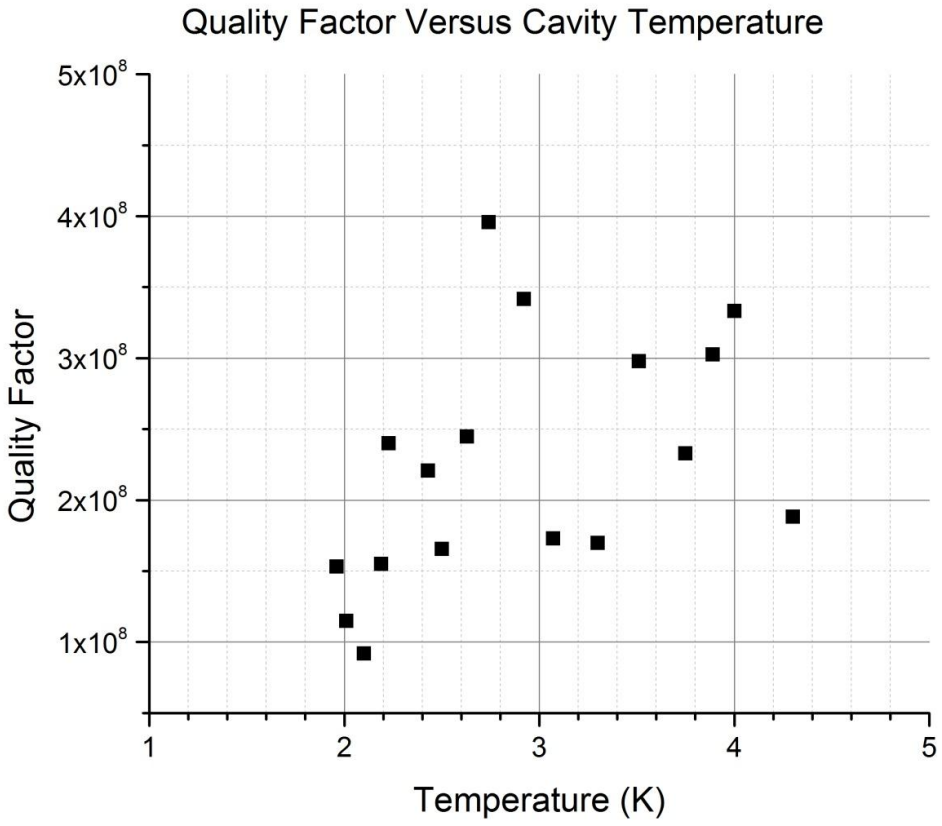

Figure 36: Quality Factor versus Cavity Temperature, Measurements Taken Using the Research RF System

The large variation in the values for the quality factor are attributed to two sources of error, first due to a mismatch in the input coupler Q_{ext} and cavity Q_0, and second due to very low power levels at which the measurements were done. This makes

the Q_0 of the cavity is effectively flat between 4K and 2K, with a value of 2-3 x 10^8, shown in Figure 36. Another interesting result was the frequency going down between 4 K and 2 K, shown in Figure 37, which is likely attributed to the pressure change when going below 4 K.

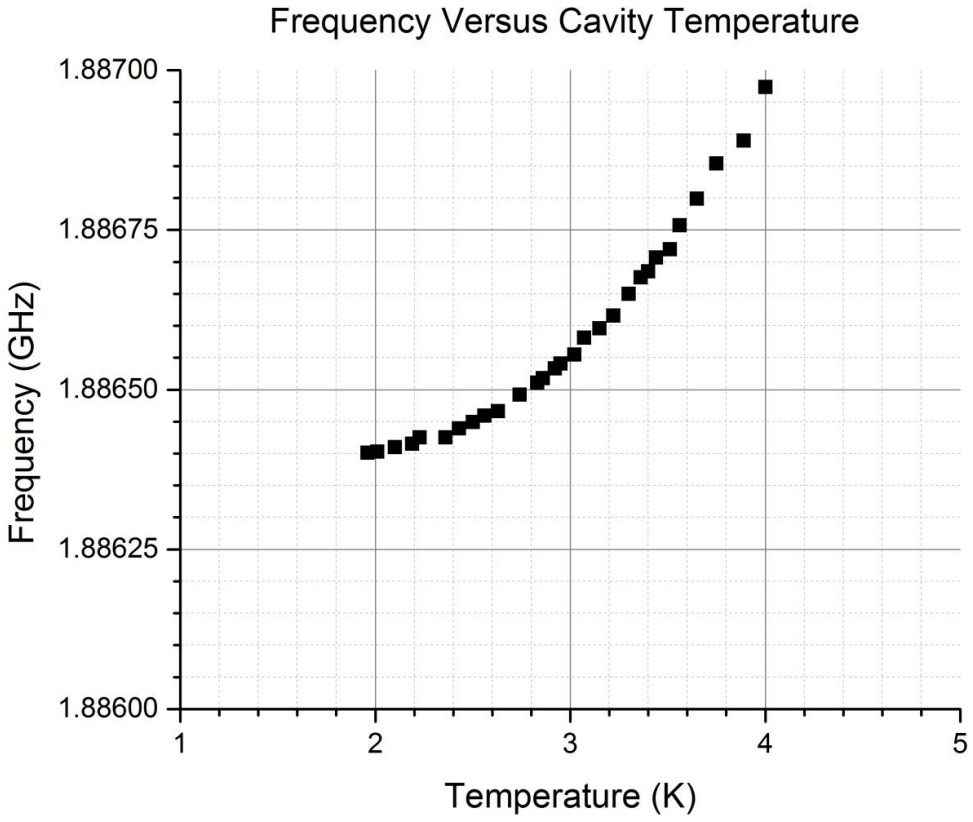

Figure 37: Frequency versus Cavity Temperature From 4.23 K to 2 K Using the Frequency on the Research RF System

IV.III.III. Low Power Level Quenching

At 2 K, the power was raised and it was noticed that the cavity was quenching at a low power level. Looking at the transmitted power, it could be seen that before the cavity could fill, it would quench. The filling was occurring on a short time scale 2-3 ms, with the quench taking on the order of μs. In the pulsed mode, even with a period between pulses of 8-10 ms the cavity was quenching. This led us to believe the cavity was quenching and then cooling again very rapidly and then quenching again.

IV.III.IV. Q Degradation

At the power levels close to where quenching occurred, the quality factor of the cavity would degrade on the time scale of a few seconds. This was attributed to heating of the sapphire, which produced higher losses. This heating occurs because of the relatively long thermal path from the high field region of crystal and the thermal bath at the top of the crystal, approximately 7 inches. The degradation of the output power can be seen in a normal fill and decay cycle in Figure 38 and the degraded fill and decay cycle shown in Figure 39. Again this effect is attributed to the time that it takes the crystal to transfer the heat dissipated due to RF heating. This effect takes roughly 4-6 seconds to begin, with an incident power level of 100 mW.

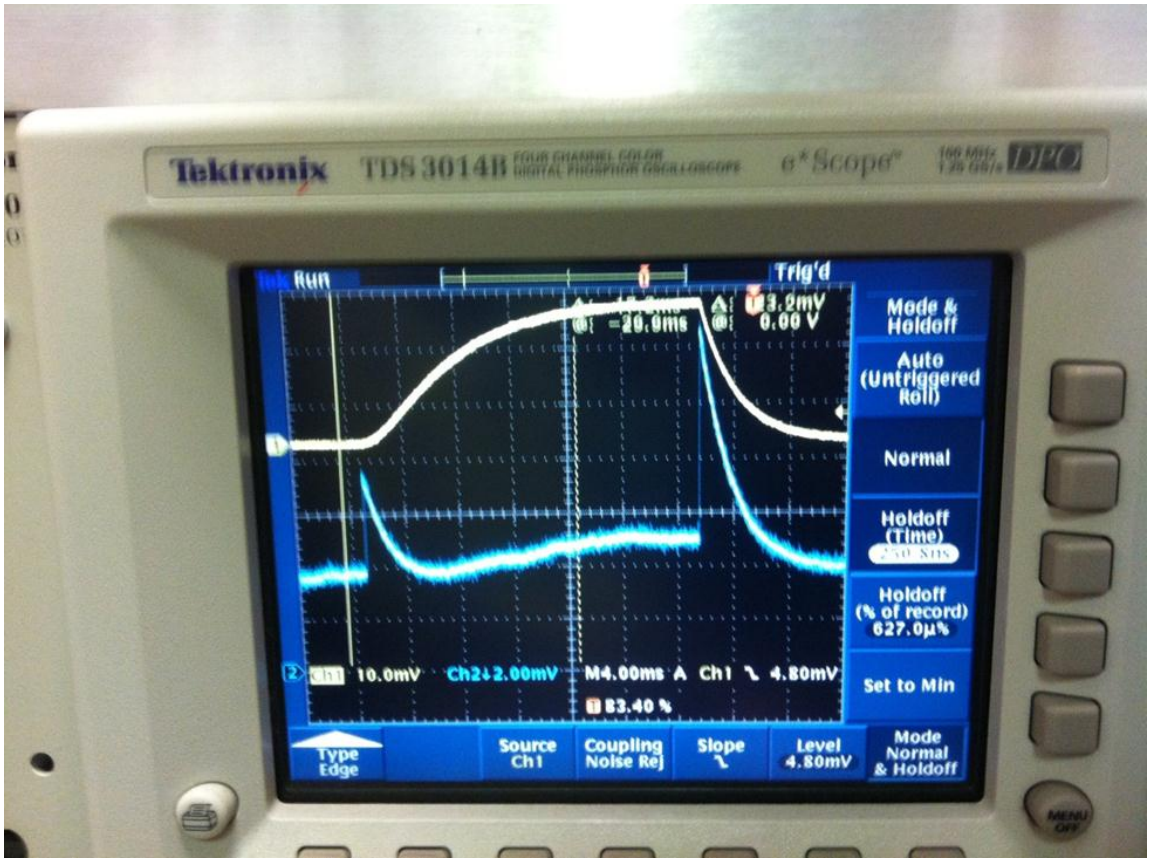

Figure 38: Normal Filling Cycle for the Wafer Test Cavity with the Reflected Power (Blue Line) and Transmitted Power (Yellow Line) Plotted Versus Time

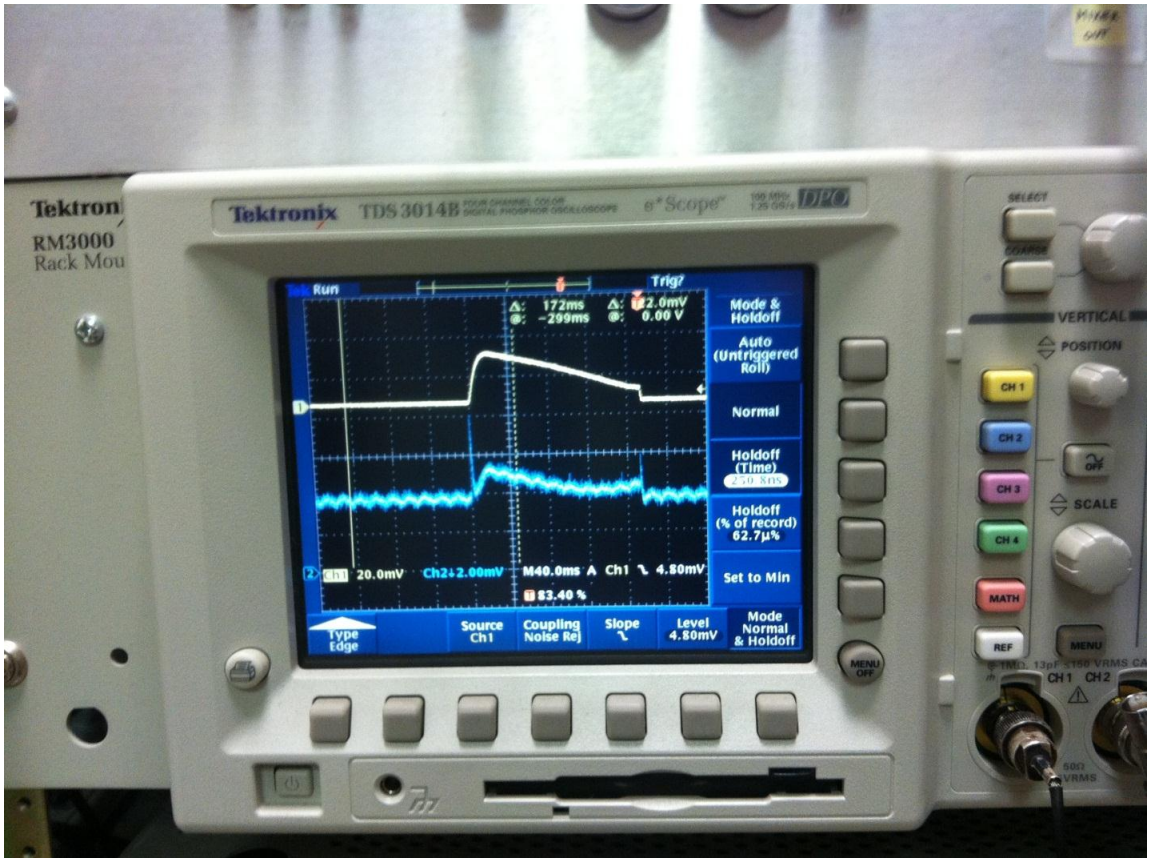

Figure 39: Degraded Filling Cycle for the Wafer Test Cavity with the Reflected Power (Blue Line) and Transmitted Power (Yellow Line) Plotted Versus Time

Upon disassembly of the cavity, the couplers were removed and a noticeable discoloration of the solder near the actual loop was discovered. The exact cause is unknown as it could have been from heating of the coupler due to poor conductivity through the joint. A more likely cause was that the coupler was multipacting with the wall of the cavity. A picture of the discolored coupler is shown in Figure 40.

Figure 40: The Loop Couplers Used in the Second Cold Test. The Probe Coupler (Top) Remained the Way It was Installed, the Input Probe (Bottom) Was Discolored Significantly

The second test provided data on the quality factor of the wafer test cavity, but it also revealed a serious problem with regard to the low power level quenching. The source of this low field quenching is not known precisely, but it is theorized that the cavity is multipacting. This multipacting could be either in the coupler tubes or in the main body of the cavity. Suggestions were made that perhaps by using a coaxial line inside the coupler tube that we were creating a high field region where it was not intended. It was decided at that time to revert back to a hook type coupler and to retest the cavity.

IV.IV. Third Cold Test

The couplers were switched to hook type couplers after the results of the second test indicated low-field multipacting and loop coupler discoloration. The original hooks were manufactured at Texas A&M University by Nick Diaczenko, to the specifications of Haipeng Wang's simulations, done using CST Microwave Studio. The couplers were set with an input Q_{ext} of $3x10^9$ and an output Q_{ext} of $1x10^{10}$. The couplers were then shipped to Ari Palczewski, at TJNAF, to be installed and have the coupling checked. The couplers were determined to have incorrect coupling and had to be modified. For simplicity, the couplers were turned down to a more manageable diameter and shortened to get the desired coupling. The cavity then underwent a 3 μm BCP and UHV cleaning, before being reassembled.

This test was performed without thermistors, as the last iteration yielded no useable data over what the Dewar's temperature monitor provided. The temperature of the bath next to the cavity was monitored by one thermistor installed on the test stand. Temperature and Q tracking was not performed on cool-down due to a lack of equipment on the test stand used. The cryogenics plant at TJNAF was having significant issues when the test was scheduled to take place. Due to time constraints the test had to continue, but reduced the available measurement equipment.

At 4.3 K the pressure instabilities in the Dewar prevented useful data from being taken, except for a data point taken by Gigi Ciovati, which was not reproducible. The issue was that the research RF system has a BW of 5 kHz for tracking a signal and the fluctuations in frequency from pressure instabilities was on the order of 20 kHz. In the 2

K range several data points were taken and reasonable results for Q_0 and the Q_{ext}'s were obtained. The general trend was rising Q with power until a plateau was reached on the transmitted power, shown in Figure 41. This is arguably due to the sapphire heating and absorbing input power. The issue with this assumption is that the power plateau did not change at all with pulse length, which seems to indicate that this is a phenomenon is due to the cavity and not the crystal. Some initial guesses were made that perhaps the coupler is multipacting on two normal conducting surfaces, which would give the power plateau and would not quench the cavity.

IV.V. Fourth Cold Test

The cavity was tested a final time, after undergoing a 120°C bake for 48 hours, while under vacuum. This was done in the hope that if the cavity was contaminated a final measurement could allow for higher field data. The test was performed by Ari Palczewski at TJNAF; unfortunately it did not offer any illumination over the previous 2 cold tests. The quality factor ranged from 1.5×10^7 to 1.5×10^8 and the transmitted power showed another plateau, shown in Figure 42. The conclusion was made that the cavity is experiencing low power level multipacting, which is likely within the cavity itself.

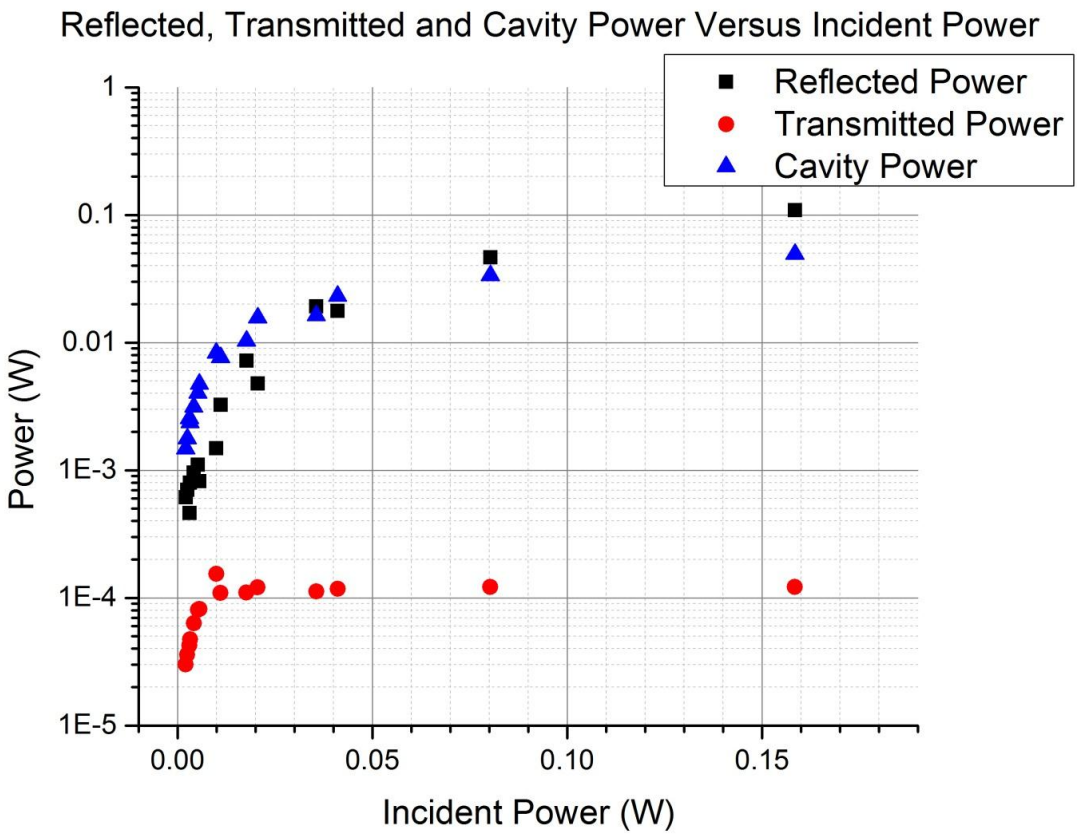

Figure 41: Reflected, Transmitted and Cavity Power versus Incident Power

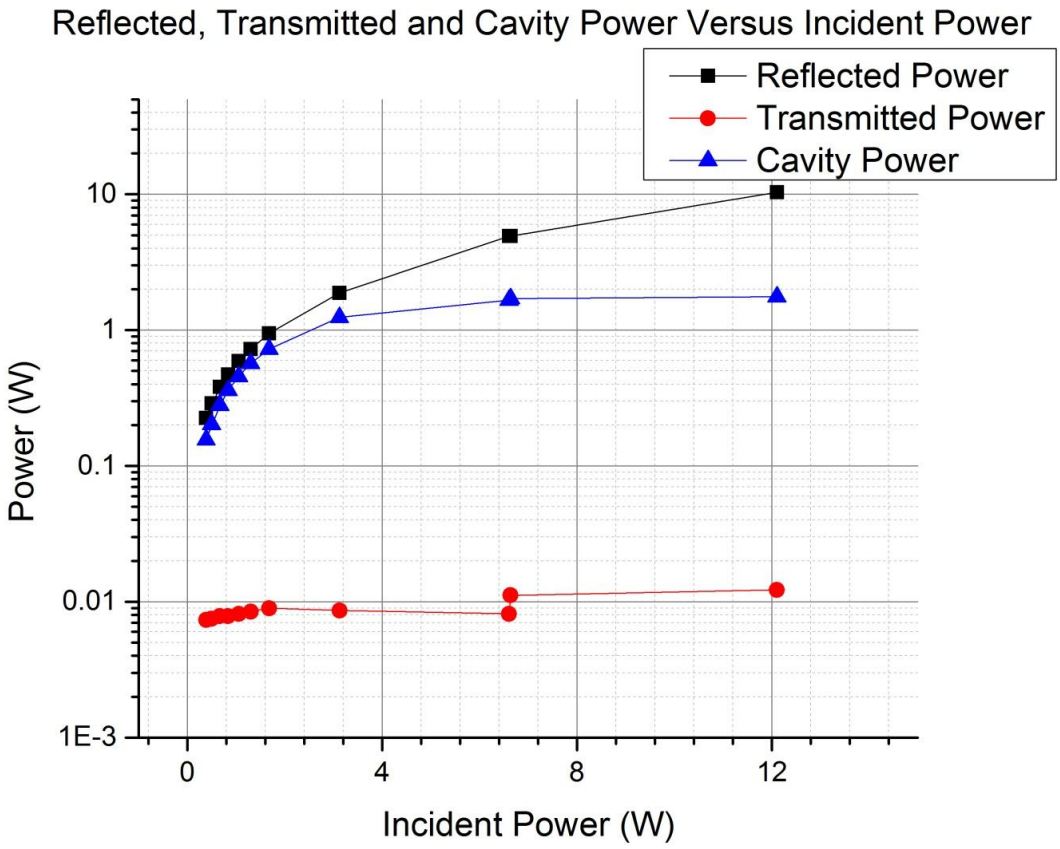

Figure 42: Fourth Test Reflected, Transmitted and Cavity Power versus Incident Power

V. RESULTS AND CONCLUSION

V.I. Simulation Results

The simulation of the wafer test cavity has shown that the cavity can achieve a maximum sample RF magnetic field of 162 mT, with a pulse length of 2 ms at 500 W. The original design of the cavity was to achieve fields on the sample above the BCS limit. The limiting factor is currently the loss tangent of the cavity and according to the values attained by other groups and presented in [11], the potential for better performance is achievable. Assuming a factor of two improvement over the measured loss tangent of the Hemex sapphires acquired from Crystal Systems a maximum field of 201 mT is possible.

V.II. Experimental Results

Testing of the wafer test cavity has yielded useful data and confirmed that the cavity has the predicted mode structure and resonant frequency. A quality factor of 3.96×10^8 has been measured with a resonant frequency of 1.886492 GHz at a temperature of 2.74 K. The coupling strategy of the cavity still requires development, as it appears that the couplers are multipacting with the walls of the coupling tubes. It is also possible that the cavity is multipacting in the bulk volume, which can be caused by a breakup of the cylindrical symmetry. The multipacting ultimately limited the amount of information that could be derived from the testing to this date.

V.III. Conclusion

The simulation results show that the cavity can be a valuable tool for the testing of superconducting materials, as it would provide significant improvement over the current maximum RF magnetic field of approximately 60 mT. Several issues persist with the coupling strategy and the potential multipacting in the cavity. Despite several tests attempting to fix the issue with the coupling issues with the cavity, development is still required. Using the simulation techniques above and the parameters acquired from the experimental testing, a value of 6.65 mT RF magnetic field has been generated in the wafer test cavity. After only 3 cryogenic tests of the cavity, this is an encouraging result.

This testing and simulation has shown that a dielectrically loaded test cavity has the potential to provide a mechanism for the future development of superconducting Heterostructures and superconducting materials.

REFERENCES

1. *The International Linear Collider: Accelerator Baseline Design*. Technical design report, Geneva, Switzerland, 2013. **3**, http://www.linearcollider.org/ILC/TDR Retrieved 5/5/2014

2. J. Preble, J.H., F. Marhauser, R. A. Rimmer, H. Wang *JLAB Upgrade and High Current Cavity Developments*. Proceedings of SRF2009, Berlin, Germany, 2009. 17-19, http://accelconf.web.cern.ch/accelconf/SRF2009/papers/moobau02.pdf. Retrieved 5/5/2014

3. S-H Kim, R.A., W. Blokland, M. Champion, A. Coleman, M. Crofford, B. DeGraff, M. Doleans, D. Douglas, T. Gorlov, B. Hannah, M. Howell, Y. Kang, S-W. Lee, C. McMahan, T. Neustadt, S. Ottaway, C. Peters, J. Saunders, A. Shishlo, S. Stewart, W.H. Strong, D. VandyGriff *The Status of the Superconducting Linac and SRF Activities at SNS*. Proceedings of SRF2013, Paris, France, 2013. 83-89, http://ipnweb.in2p3.fr/srf2013/papers/mop007.pdf. Retrieved 5/5/2014

4. D. Boussard, T.L. *The LHC Superconducting RF System*. CEC-ICMC'99, Montreal, Canada, 1999. http://cds.cern.ch/record/410377/files/lhc-project-report-316.pdf?origin=publication_detail. Retrieved 5/5/2014

5. Jensen, M.R.F. *Operational Experience with SRF Cavities for Light Sources*. Proceedings of SRF2011, Chicago, IL, 2011. http://accelconf.web.cern.ch/accelconf/SRF2011/papers/moiob05.pdf. Retrieved 5/5/2014

6. K. Honkavaara, B.F., J. Feldhaus, S. Schreiber, R. Treusch *Status of the Free-Electron Laser User Facility FLASH*. Proceedings of SRF2009, Berlin, Germany, 2009. 1-5, http://accelconf.web.cern.ch/accelconf/SRF2009/papers/mooaau01.pdf. Retrieved 5/5/2014

7. A. Nagler, I.M., D. Berkovits, K. Dunkel, M. Pekeler, C. Piel, P. vom Stein, H. Vogel *Status of the SARAF Project*. Proceedings of LINAC 2006, Knoxville, Tennessee, 2006. http://accelconf.web.cern.ch/accelconf/l06/PAPERS/MOP054.PDF. Retrieved 5/5/2014

8. J. Arthur, U.B., A. Brunger, C. Bostedt, S. Boutet, J. Bozek, D. Cocco, T. Devereaux, Y. Ding, H. Dürr, D. Fritz, K. Gaffney, J. Galayda, J. Goldstein, M. Gühr, J. Hastings, P. Heimann, K. Hodgson, Z. Huang, N. Kelez, P. Montanez, A. Robert, M. Rowen, W. Schlotter, M. Seibert, J. Stöhr, J. Turner, W. White, J. Wu, G. Williams, V. Yachandra, J. Yano *Science Driven Instrumentation for LCLS-II: A White Paper outlining science and scope of instrumentation*. White Paper, Stanford, California, 2012. 1-92, https://portal.slac.stanford.edu/sites/lcls_public/Instrument_Document_Repository/LCLS-II_Instrumentation_Whitepaper_DOE.pdf. Retrieved 11/20/2012

9. M. Altarelli, R.B., M. Chergui, W. Decking, B. Dobson, S. Düsterer, G. Grübel, W. Graeff, H. Graafsma, J. Hajdu, J. Marangos, J. Pflüger, H. Redlin, D. Riley, I. Robinson, J. Rossbach, A. Schwarz, K. Tiedtke, T. Tschentscher, I. Vartaniants, H. Wabnitz, Hans Weise, R. Wichmann, K. Witte, A. Wolf, M. Wulff, M. Yurkov *The European X-Ray Free-Electron Laser*. Technical design report, 2007. 1-646, http://xfel.desy.de/technical_information/tdr/tdr/. Retrieved 5/5/2014

10. K.Saito *Critical Field Limitation of the Niobium Superconducting RF Cavity*. The 10th Workshop on RF Superconductivity, Tsukuba, Japan, 2001. 583-587, https://accelconf.web.cern.ch/accelconf/srf01/papers/ph003.pdf?origin=publication_detail. Retrieved 5/5/2014

11. Pogue, N. *Wafer Test Cavity Design and Results of Dielectric Test Cavity Performance Utilizing a Ultra-Pure Sapphire*. Ph D. Dissertation in Physics, Texas A&M University, 2010

12. Pogue, N.M., P. Sattarov, A. Blackburn, R. Manus, R. Marhauser, F. Reece, C., *Superconducting RF Cavity for Testing Materials and Fabrication Processes at 1.3 GHz at Over Three Times the BCS Limit.* AIP Conference Proceedings, 2010. **1218**(1): p. 849-856 DOI: 10.1063/1.3422439.

13. Gurevich, A. *Enhancement of RF Breakdown Field of Superconductors by Multilayer Coating*. Applied Physics Letters, 2006. **88**, 1-3 DOI: 10.1063/1.2162264. Retrieved 5/5/2014

14. M. Liepe , S.P. *Nb3Sn for SRF Application*. Proceedings of SRF2013, Paris, France, 2013. 767-770, ipnweb.in2p3.fr/srf2013/papers/weioa04.pdf. Retrieved 5/5/2014

15. T. Tajima, L.C., D.J. Devlin, R.K. Schulze, I.O. Usov, G.C. Martinez *Status of MgB2 Coating Studies for SRF Applications*. Proceedings of SRF2013, Paris, France, 2013. 771-775, http://ipnweb.in2p3.fr/srf2013/papers/weiob01.pdf. Retrieved 5/5/2014

16. XIAO, B.P. *Surface Impedance of Superconducting Radio Frequency (SRF) Materials*. Ph D. Dissertation in Department of Applied Science, College of William & Mary, 2011

17. C. Nantista, S.T., J. Weisend, R. Siemann, and V. Dolgashev *Test Bed for Superconducting Materials*. SLAC-PUB-11246, 2005. http://www.slac.stanford.edu/cgi-wrap/getdoc/slac-pub-11246.pdf. Retrieved 5/5/2014

18. L. Phillips, G.K.D., J. R. Delayen, J. P. Ozelis, and H. Wang *A Sapphire Loaded TE011 Cavity for Surface Impedance Measurements – Design, Construction, and Commissioning Status*. Twelfth International Workshop on RF Superconductivity, 2005. **441**, http://www.lns.cornell.edu/public/SRF2005/posters/tuesday/TuP46_poster_srf2005.pdf. Retrieved 5/5/2014

19. Xiao, B.P., et al. *Radio frequency surface impedance characterization system for superconducting samples at 7.5 GHz*. Review of Scientific Instruments, 2011. **82**, - DOI: doi:http://dx.doi.org/10.1063/1.3575589. Retrieved 5/5/2014

20. G. Eremeev, L.P., C.E. Reece, A.-M. Valente-Feliciano, B.P. Xiao *Characterization of Superconducting Samples with SIC System for Thin Film Developments: Status and Recent Results*. Proceedings of SRF2013, Paris, France, 2013. 593-596, http://ipnweb.in2p3.fr/srf2013/papers/tup070.pdf. Retrieved 5/5/2014

21. N. Pogue, P.M., A. Sattarov, R. Blackburn, R. Manus, F. Marhauser, C. Reece, *Superconducting RF Cavity for Testing Materials and Fabrication Processes at 1.3 GHz at Over Three Times the BCS Limit of Niobium* CEC: Advances in Cryogenic Engineering, 2009(1218): p. 849-856 DOI: http://dx.doi.org/10.1063/1.3422439.

22. Sattarov, A., *Direct Cooling (analytical model).* 2009.

23. Powers, T. *Theory and Practice of Cavity RF Test Systems*. Internal Document. http://projectx-docdb.fnal.gov/cgi-bin/RetrieveFile?docid=511;filename=ACF2B7.pdf;version=1. Retrieved 5/5/2014

24. V. B. Braginsky, V.S.I., and Kh. S. Bagdassarov *Experimental observation of fundamental microwave absorption in high-quality dielectric crystals*. Physics Letters A, 1987. **120**, 300-305 DOI: 10.1016/0375-9601(87)90676-1. Retrieved 5/1/2014

APPENDIX A

```
t1 = 2 * 10^-3; "Pulse Length";
t2 = 0.2;
r = 0.787 * 0.0254 / 2;
Q = 10 * 10^9; "Quality Factor at t0";
w = 1.19 * 10^10; "Angular Frequency of Cavity";
P0 = 500; "Input Power";
A = Pi * r^2; "Area of the Sapphire's Shaft";
L = 0.1825498; "Length of Sapphire Shaft";
c0 = 8.607 × 10^(-5) * 1.81;
"Fit Parameter for Heat Capacity, asuuming C(T)=c0*T^3";
k0 = 2.95; "Fit Parameter for Thermal Conductivity, asuuming k(T)=k0*T^3";
T0 = 2; "Initial Temperature of the Cavity";
σ = 0.62347561; "Fraction of the Energy in the Sapphire";

s[T_] := 0.00000000333305 - 0.000000000461188 * T + 0.000000000137301 * T^3 -
   0.000000000000299135 * T^5 + 7.72993 * 10^(-15) * T^6 - 5.61068 * 10^(-17) * T^7;
s1 := 1 * 10^-10;

sol1 = NDSolve[{
    E1'[t] == -w * E1[t] / (1 / (1 / Q + s[Temp[t]])) + P0,
    E2'[t] == -A * k0 * E2[t] / (L * c0) + w * s[Temp[t]] * σ * E1[t],
    Temp[t] == (4 * E2[t] / c0 + T0^4)^(1 / 4),
    E1[0] == 0, E2[0] == 0},
   {E1, E2, Temp}, {t, 0, t1}];

E1n = Flatten[Evaluate[{E1[t1]} /. sol1]][[1]];
E2n = Flatten[Evaluate[{E2[t1]} /. sol1]][[1]];

sol2 = NDSolve[{
    E1'[t] == -w * E1[t] / (1 / (1 / Q + s[Temp[t]])),
    E2'[t] == -A * k0 * E2[t] / (L * c0) + w * s[Temp[t]] * σ * E1[t],
    Temp[t] == (4 * E2[t] / c0 + T0^4)^(1 / 4),
    E1[t1] == E1n, E2[t1] == E2n},
   {E1, E2, Temp}, {t, t1, t2}];

Flatten[Evaluate[{E1[t2]} /. sol2]][[1]]
Flatten[Evaluate[{E2[t2]} /. sol2]][[1]];
```